Palaeontologia Electronica
palaeo-electronica.org

The first late middle Pleistocene *Stegodon* (Proboscidea, Stegodontidae) evidence found in Peninsular Malaysia

Amir Hakim Amiruddin, Lim Tze Tshen, Alexandra van der Geer, Kira E. Westaway, Chiang Hongwei, Ru Smith, Hijaz Kamal Hasnan, Norliza Ibrahim, Mohd Azmi Abdul Razak, Nguyen Thi Mai Huong, Nguyen Anh Tuan, and Ros Fatihah Muhammad

ABSTRACT

A maxillary left milk molar (dp3) of a *Stegodon* was discovered in a cave in northern Peninsular Malaysia. This finding represents the southernmost record of Stegodontidae in continental Asia. The half-exposed tooth was embedded in breccia attached to the cave wall. A micro-computed tomography (μCT) scanning was employed to virtually isolate the specimen from the matrix and to reconstruct a 3D model of the fossil for accurate measurements. No sign of wear or mechanical abrasion was observed in the specimen. Age determination on the matrix based on post-infrared infrared luminescence (pIR-IRSL) dating and U-series revealed a late middle Pleistocene age of between 233 ± 31 to 199 ± 28 ka. Detailed comparisons with specimens of *Stegodon orientalis* and *Stegodon trigonocephalus* revealed a number of differences in size and morphologies (development of posterior cingulum, presence of enamel tubercles at posterior cingulum, tapering of each plate lingual-buccally, thickness of the plates, and depth of the valley between plates) which are different to either of these species. The discovery of *Stegodon* in Peninsular Malaysia provides a better understanding of the distribution of this genus in the Sundaic subregion during the middle Pleistocene.

Amir Hakim Amiruddin. Department of Geology, Universiti Malaya, 50603, Kuala Lumpur, Malaysia.
amirhakim081197@gmail.com
Lim Tze Tshen. Department of Geology, Universiti Malaya, 50603, Kuala Lumpur, Malaysia.
limtzetshen@yahoo.com
Alexandra van der Geer. Naturalis, Darwinweg 2, 2333 CR Leiden, Netherlands.
alexandra.vandergeer@naturalis.nl
Kira E. Westaway. School of Natural Sciences, Faculty of Science and Engineering, Macquarie University,

Final citation: Amiruddin, Amir Hakim, Lim, Tze Tshen, van der Geer, Alexandra, Westaway, Kira E., Hongwei, Chiang, Smith, Ru, Hasnan, Hijaz K., Ibrahim, Norliza, Razak, Mohd Azmi Abdul, Nguyen, Thi Mai Huong, Nguyen, Anh Tuan, and Muhammad, Ros Fatihah. 2025. The first late middle Pleistocene *Stegodon* (Proboscidea, Stegodontidae) evidence found in Peninsular Malaysia. Palaeontologia Electronica, 28(3):a43.
https://doi.org/10.26879/1432
palaeo-electronica.org/content/2025/5637-stegodon-in-peninsular-malaysia

NSW 2109, Australia. kira.westaway@mq.edu.au
Chiang Hongwei. Research Center for Environment Changes, Academia Sinica Taipei 115201, Taiwan, ROC. hwchiang@ntu.edu.tw
Ru Smith. Department of Geology, Universiti Malaya, 50603, Kuala Lumpur, Malaysia. ru.d.a.smith@gmail.com
Hijaz Kamal Hasnan. Department of Geology, Universiti Malaya, 50603, Kuala Lumpur, Malaysia. hijazzains@um.edu.my
Norliza Ibrahim. Department of Oral & Maxillofacial Clinical Sciences, Faculty of Dentistry, Universiti Malaya, 50603 Kuala Lumpur, Malaysia. norlizaibrahim@um.edu.my
Mohd Azmi Abdul Razak. Department of Restorative Dentistry, Faculty of Dentistry, Universiti Malaya, 50603 Kuala Lumpur, Malaysia. azmirazak@um.edu.my
Nguyen Thi Mai Huong. Institute of Archaeology, Hanoi, Vietnam. maihuong72@gmail.com
Nguyen Anh Tuan. Institute of Archaeology, Hanoi, Vietnam. nguyenanhtuanvkch@gmail.com
Ros Fatihah Muhammad. Department of Geology, Universiti Malaya, 50603, Kuala Lumpur, Malaysia (corresponding author). rosfmuhammad@um.edu.my

Keywords: juvenile; karst fossil; 3D computed tomography; Quaternary; luminescence dating

Submission: 23 July 2024. Acceptance: 27 August 2025.

INTRODUCTION

The genus *Stegodon* is a key taxon in the studies of the Pleistocene mammalian faunas in mainland Southeast Asia and south China that were characterized by the occurrence of the early to late Pleistocene faunal assemblage *"Ailuropoda–Stegodon* faunal complex" (Kahlke, 1961; Rink et al., 2008; Suraprasit et al., 2016).

Fossil records suggested that this genus was widely distributed in parts of central and east Africa and south and Southeast Asia. Thus far, fossils recorded from mainland and insular Asia were reported from China, Taiwan, Japan, India, Pakistan, Nepal, Myanmar, Thailand, Laos, Vietnam, Indonesia and Philippines, with ages ranging from the late Miocene to the late Pleistocene or Holocene (O' Reagan et al., 2005; Ao et al., 2016). Miocene and Pliocene representatives of the genus in Asia such as *S. zhaotongensis, S. licenti, S. clifti, S. bombifrons, S. zdanskyi, S. officinalis, S. aurorae, S. miensis,* and *S. insignis* were found in east and south Asia, with the exception of *S. sompoensis*, which was recorded only in Sulawesi island (Indonesia); later forms, including *S. chiai, S. huananensis, S. wushanensis, S. preorientalis, S. sinensis,* and *S. elephantoides* were found from earlier Pleistocene deposits in China, Taiwan, Myanmar, and Laos, with no known records dated later than that. Large- and medium-sized *Stegodon*, such as *S. orientalis* and *S. trigonocephalus*, as well as dwarf species *(S. hypsilophus, S. sumbaensis, S. timorensis, S. sondaari, S. florensis,* and *S.* cf. *luzonensis)* thrived in various places in continental and insular Southeast Asia (including, Sundaic subregion in the west and Wallacea in the east) and Luzon island in the Philippines during the middle Pleistocene times. Even though *S. orientalis* and *S. trigonocephalus* were known to have existed in earlier Pleistocene, these two species persisted through middle Pleistocene until at least to the late Pleistocene (Table 1). The genus was generally recorded as globally extinct during terminal Pleistocene (van den Bergh et al., 2008; Turvey et al., 2013), with a few controversial Holocene records from mainland China (Tong and Liu, 2004).

Locations of middle to late Pleistocene sites in mainland Southeast Asia and Java are shown in Figure 1. Within the Malay Peninsula, the geographically closest known occurrence of *Stegodon* is from Satun province in peninsular Thailand (Duangkrayom et al., 2017). However, as of the time of this study, those specimens have not yet been dated. This is an in-depth analysis of a *Stegodon* fossil found from a cave in northern Peninsular Malaysia. The finding was briefly reported by Muhammad et al. (2020) and represents the southernmost distribution of the genus in mainland Southeast Asia.

The present work aims to provide a detailed description of the new *Stegodon* fossil from Peninsular Malaysia based on µCT scans. We also report the results of the geochronological dating based on pIR-IRSL dating of feldspar grains from the surrounding breccia matrix and U-series of a flowstone that overlies the *Stegodon* fossil, in this new Pleistocene fossil site in Malaysia.

TABLE 1. The First Appearance Datum (FAD) and Last Appearance Datum (LAD) records of *Stegodon* species from China, Taiwan, Japan, India, Pakistan, Nepal, and Southeast Asia.

Species	FAD	LAD	Place	Source
Stegodon orientalis	early Pleistocene (1.5 Ma)	Holocene(?)	China Japan Vietnam Laos Thailand	Lin, 1963; Konishi and Otsuka, 1984; An et al., 1990; Ma and Tang, 1992; Long et al., 1996; Saegusa, 1996; Yoshikawa, 1999; Tong and Patou-Mathis, 2003; Tong and Liu, 2004; Saegusa et al., 2005; Bacon et al., 2011; Duangkrayom, 2018; Chen, 2021
S. zdanskyi	Pliocene	Unknown	China	Hu, 1962; Chen, 2021
S. chiai	early Pleistocene	Unknown	China	Chen, 2021
S. zhaotongensis	late Miocene	early Pliocene	China	Chen, 2021
S. officinalis	Pliocene(?)	Unknown	China	Chen, 2021
S. licenti	late Miocene	Pliocene	China	Chen, 2021
S. huananensis	early Pleistocene (2.6 Ma to 1.8 Ma)	Unknown	China	Sun et al., 2014; Chen, 2021
S. wushanensis (?)	early Pleistocene	Unknown	China	Chen, 2021
S. preorientalis	early Pleistocene	Unknown	China	Louys et al., 2007
S. aurorae	late Pliocene (2.5 Ma)	early Pleistocene (1.0 Ma)	Japan Taiwan	Shikama et al., 1975; Takashi et al., 2001
S. miensis	late Pliocene	Unknown	Japan	Aiba et al., 2006
S. sinensis	early Pleistocene	Unknown	China Taiwan Laos	Arambourg and Fromaget, 1938; Otsuka, 1984; Chen, 2021
S. elephantoides	early Pleistocene	Unknown	China Myanmar	Clift,1828; Louys et al., 2007
S. clifti	late Miocene	early Pliocene	India Pakistan	Falconer and Cautley, 1847; Falconer, 1857
S. khet-puralensis	Unknown	Unknown	India	Nanda, 1980
S. kartiliensis	Unknown	Unknown	India	Nanda, 1980
S. pinjorensis	Unknown	Unknown	India	Osborn, 1929
S. insignis (Synonym: *S. ganesa)*	late Pliocene (2.48 Ma)	Unknown	Nepal India Myanmar	Osborn, 1942; Sharma and Singh, 1966; West and Munthe, 1981; Corvinus, 1988; Nanda, 1988; Kundal et al., 2017
S. bombifrons	late Miocene	Unknown	Nepal India Pakistan	Falconer and Cautley, 1847; Corvinus, 1988; Zong, 1995; Aslam et al., 2015
S. hypsilophus	middle Pleistocene	Unknown	Java	Hooijer, 1954; van den Bergh, 1999
S. trigonocephalus	early Pleistocene (1.2 Ma)	late Pleistocene (300 ka)	Java	van den Bergh, 1999, 2001, 2008
S. sompoensis	late Pliocene (2.5 Ma)	early Pleistocene	Sulawesi	de Vos et al., 2007
S. florensis	middle Pleistocene	late Pleistocene (460 ka)	Flores	van den Bergh, 1999, 2022
S. sumbaensis	middle Pleistocene	late Pleistocene	Sumba	van der Geer et al., 2016
S. timorensis	middle Pleistocene (710 ka)	late Pleistocene (130 ka)	Timor	Louys et al., 2016; Jensen et al., 2017
S. sondaari	early Pleistocene (1.4 Ma)	middle Pleistocene (700 ka)	Timor	van den Bergh, 2008, 2022
S. cf. *luzonensis*	middle Pleistocene (727 ± 30 ka)	Unknown	Luzon	Ingicco et al., 2018; Lambard et al., 2024
S. mindanensis	Unknown	Unknown	Mindanao	Naumann, 1890

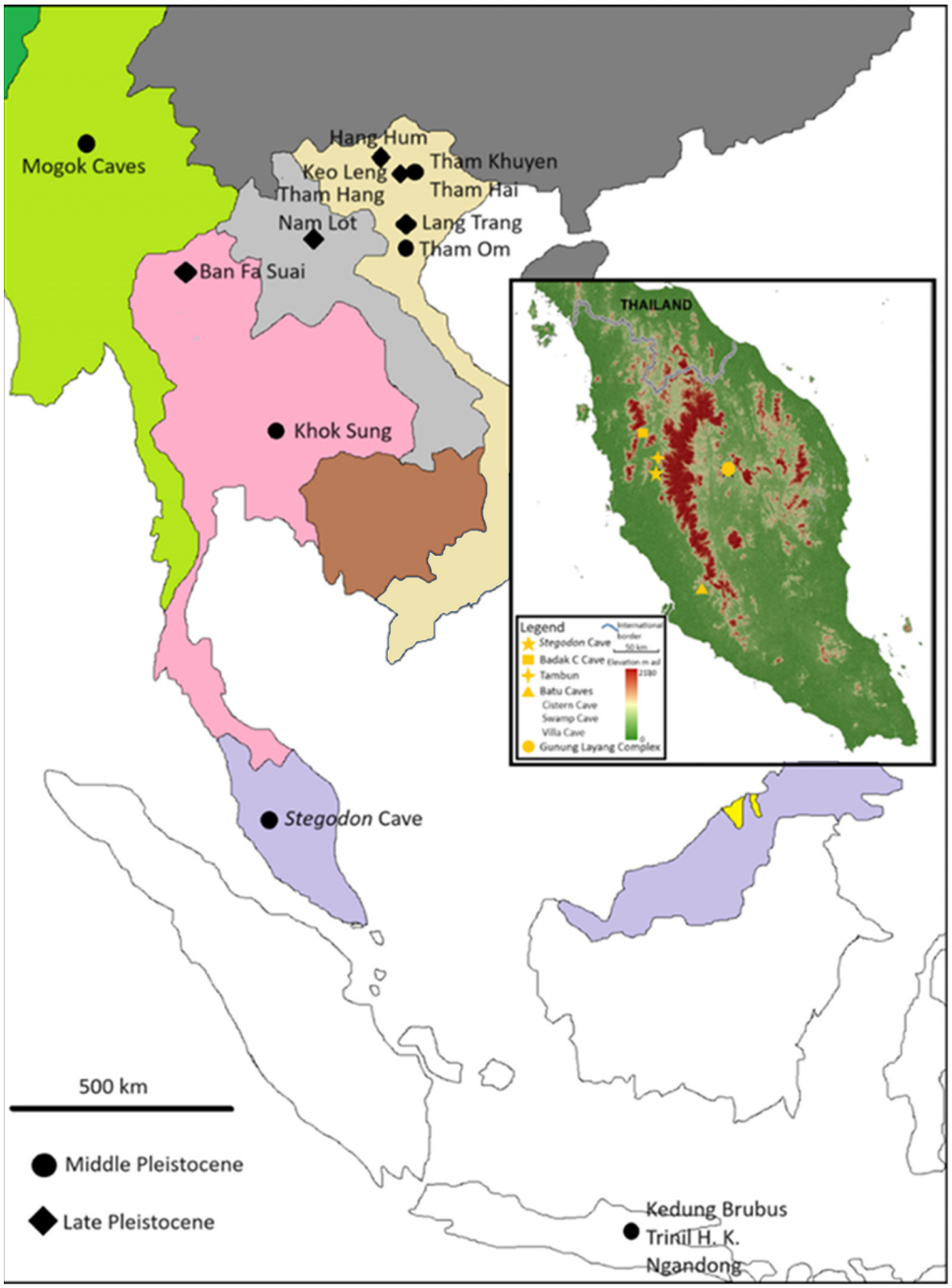

FIGURE 1. Map of Southeast Asia showing the locations of middle and late Pleistocene *Stegodon* sites. The middle Pleistocene sites include, Khok Sung, in Thailand (Suraprasit et al., 2016), Mogok Caves in Myanmar (Takai et al., 2006), Tham Om, Tham Khuyen, and Tham Hai in Vietnam (Ciochon, 2009). The late Pleistocene sites include Ban Fa Suai, in Thailand (Zeitoun et al., 2005, 2010), Nam Lot and Tham Hang South, in Laos (Bacon et al., 2008, 2011, 2012, 2015), Hang Hum, Keo Leng (Olsen and Ciochon, 1990), and Lang Trang (de Vos and Long, 1993; Long et al., 1996) in Vietnam. The insular *Stegodon* sites in Kedung Brubus, Trinil H.K (Hauptknochenschicht) (van den Bergh, 2001) and Ngandong (Tougard, 2001) are dated middle Pleistocene. Insert shows shaded relief map of Peninsular Malaysia with location of *Stegodon* Cave on the west of the Main Range batholith that forms the main highland. All key cave fossil sites like Tambun (Hooijer, 1963), Badak C Cave, Naga Mas Cave and Batu Caves (Ibrahim et al., 2013) are located on the west side of the highlands, with a new site of Gunung Layang complex on the east (Muhammad et al., 2019). Source: Shuttle Radar Topography Mission (SRTM) Digital Elevation Model (DEM) data with a resolution of 1-arc second (~30 m), courtesy of the U.S. Geological Survey, generated using ArcGIS.

GEOLOGICAL SETTING

The study area is located in Gopeng (Kinta Valley), a district in the state of Perak, about 180 km north of Kuala Lumpur in the west part of Peninsular Malaysia (04°28'16.1503", 101°08'57.4313") at 50 m above mean sea level (Figure 1). The small hill and cave network where the *Stegodon* fossil was found were previously unmarked on regional topographical maps consulted (Muhammad et al., 2020). The cave was subsequently named *Stegodon* Cave, and this name will be used in this article.

The karst system in the valley consist of the ± 1550 m thick Kinta Limestone that was earlier assigned a Lower Devonian to Middle Permian age (Suntharalinggam, 1968) and later a Middle Ordovician to Middle Permian age (Henri and Amnan, 1994). It forms typical tropical karst towers that protrude above the vast valley (Muhammad, 2018) while most of it in the form of dissected subsurface platforms. The valley is sandwiched in between two I-type granitic highlands (Ghani et al., 2013), the Main Range in the east and Kledang Range on the west. Heavy drainage from the highlands brought down the alluvium, the products of weathered granite into the floodplain. Walker (1965) named the main stratigraphic units of the Cenozoic cover in Kinta Valley as Boulder Beds, Old Alluvium and Young Alluvium. The sediments were reassessed and Old Alluvium renamed as Simpang Formation and Young Alluvium as Beruas Formation by Suntharalinggam (1983).

The tin-rich alluvium that blankets the valley is associated with the Simpang Formation while the younger Beruas Formation fills up V-shaped valleys. Even though the earlier Simpang Formation was assigned to the Pleistocene, the underlying Cenozoic sediments that cannot be differentiated from the Quaternary sediments (Suntharalinggam, 1983) imply that this formation could extend into the Neogene. This has also been indicated earlier by Batchelor (1979a, 1979b).

Stegodon Cave

This cave forms a single northeast-southwest orientated 94 m passage that cuts through the small unnamed karst hill, with its floor located about 6 m above the general ground. The average height of the ceiling is about 2 m throughout the cave, and width of not more than 10 m. Two distinctive vertical shafts connect the passage to the lower passage, which lies on the general ground (Figure 2).

Remnants of highly lithified breccia up to 80 cm thick line both walls, and certain parts over the speleothems. The breccia is oligomictic, and primarily comprises fine sands with some muds, along with streaky crystalline carbonate intercalations and a few subangular rock pebbles. The tooth of the *Stegodon* was located about 16 m from the northeast mouth, on the northwestern wall, approximately 70 cm above the floor (Figure 3). Scattered fossil-bearing unconsolidated sediments embed the walls and ceiling of the lower passage.

MATERIALS AND METHODS

Abbreviations

PRK Perak, Malaysia

SC *Stegodon* Cave

KL Keo Leng, Vietnam

LKCNHM Lee Kong Chian Natural History Museum, National University of Singapore, Singapore.

LF Lamellar frequency

Description and measurements of the *Stegodon* tooth

Results from visual observation of the external morphological characters were documented. A complete cave passageway was mapped and drawn using simple traversing with laser rangefinder and a compass.

All measurements were taken using handheld vernier callipers (model: H+W: 150 x 0.05mm) for the width of the plates, length and height of the molars. Morphological terms for cheek teeth and methods of measuring and tabulating biometrical parameters are largely based on those used by Maglio (1973: 8-13), Roth and Shoshani (1988: 572-574) and van den Bergh (1999: 28-30). Dimensions used in the measurement include:

Length (L) – Maximum length of a cheek tooth, measured along the longitudinal axis of the tooth parallel to crown base.

Width (W) – Maximum width of a cheek tooth, measured across the widest plate (including the covering cementum layer, if any) with the jaws of the calliper parallel to the anterior and posterior plates.

Height (H) – Maximum height of the highest plate, measured from crown base (not including root mass) to the top of the plate.

Height/Width Index (H/W Index) – Also known as Hypsodonty Index (HI) or Relative Crown Height (RCH), in which the maximum height (H) of a tooth

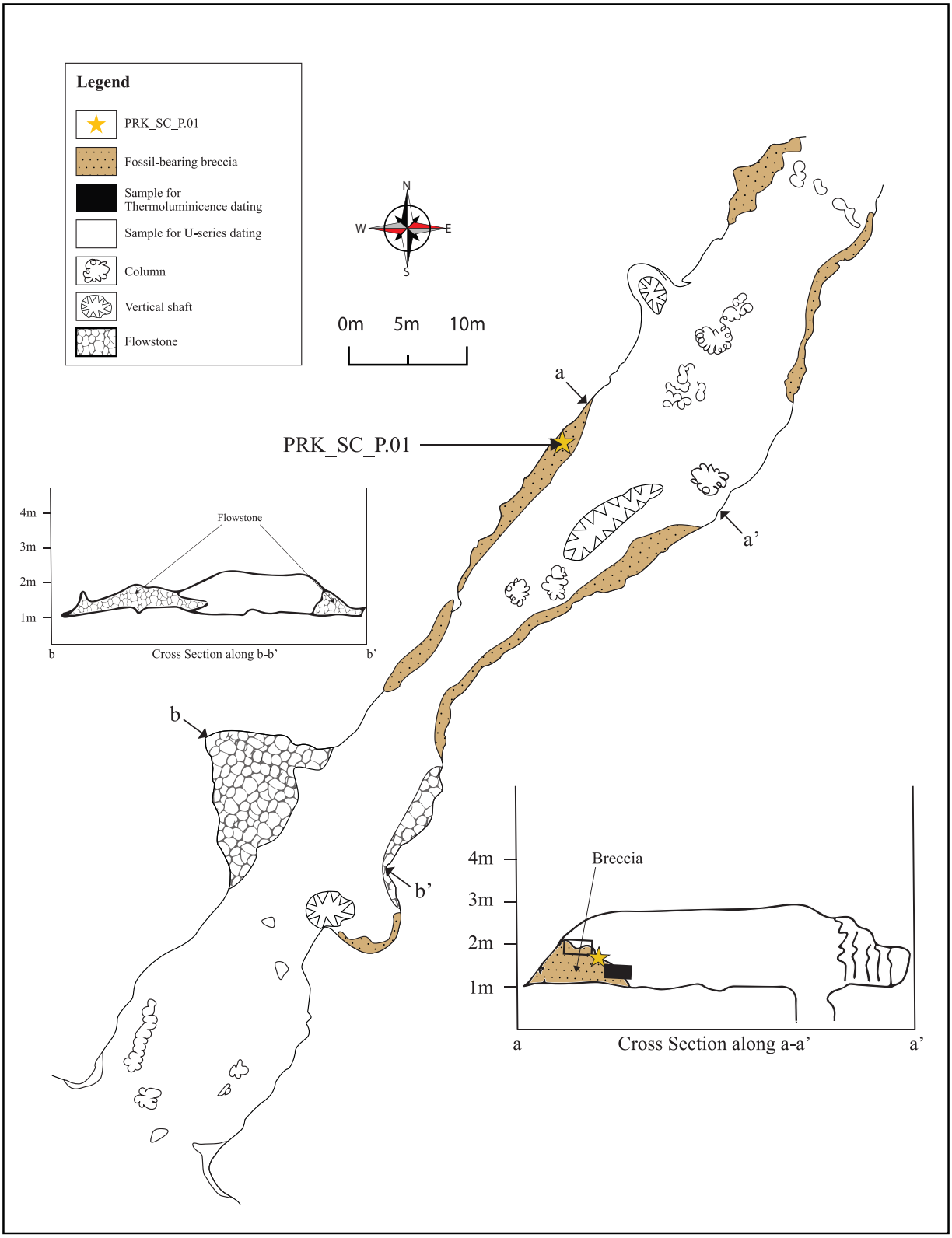

FIGURE 2. Cave map and cross-sections of *Stegodon* Cave along with locations of the *Stegodon* fossil (PRK_SC_P.01) and dating samples.

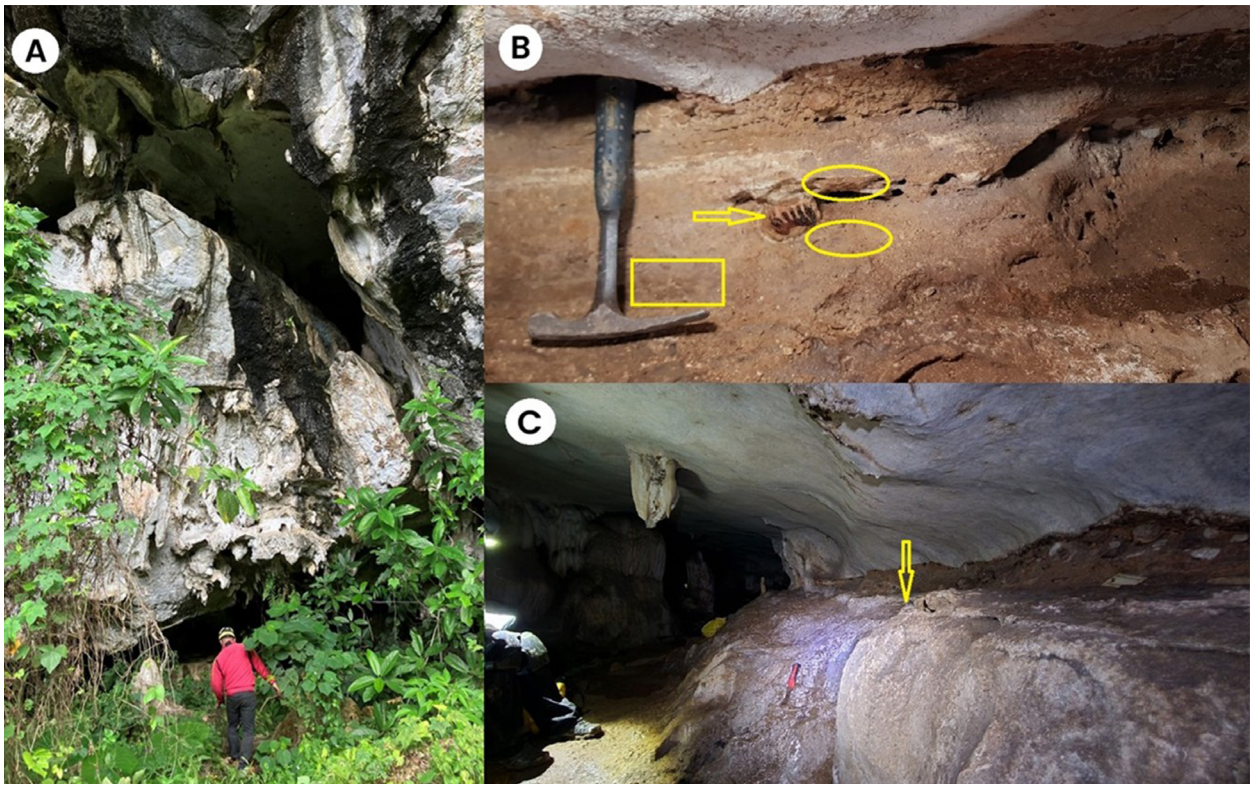

FIGURE 3. Field photos: A: northeastern entrance of the cave located about 6 m from the ground, B: showing the fossil (arrow), samples for U-Th dating (ovals) and luminescence dating (square), C: location of the fossil (arrow) about 70 cm from the cave floor, and 20 m from the northeastern entrance of the cave.

is expressed as a percentage of its maximum width (W) and calculated by multiplying the height-width ratio by 100.

Plate number or Plate formula – The total number of plates or lamellae present or preserved as viewed from the side of a tooth which includes the small half-plate at the front end of a tooth and also plates partially covered within cementum.

Lamellar Frequency (LF) – (Total number of plates x 100)/ Maximum length.

This paper follows the common practice among modern palaeontologists to label the six cheek teeth of *Stegodon* and *Elephas* specimens as dp2-dp3-dp4-M1-M2-M3, instead of using Roman numerals I to VI, to indicate the order of the tooth growth from the back to the front of each jaw quadrant.

The *Stegodon* specimen (Catalogue No.: PRK_SC_P.01) is temporarily housed in the Geology Department of Universiti Malaya. Direct comparisons were made with one specimen of *S. orientalis* from Keo Leng, Vietnam (Institute of Archaeology, Hanoi) and one specimen of *S. trigonocephalus* (CD 11649) from Java, Indonesia (Naturalis Biodiversity Center, Leiden). The *S. orientalis* specimen from Vietnam does not seem to have any catalogue number, so it is here referred to as 'KL DP3'. Both of these comparative fossil specimens have been identified as maxillary milk teeth (dp3). For lamellar frequency comparison we also used a selected group of fossil and modern dp3s: *Stegodon trigonocephalus*, CD 11647a and CD 11647b (from Hooijer, 1955), and modern Asian elephant *Elephas maximus*, ZRC 4.1669 from the Lee Kong Chian Natural History Museum, Singapore.

Terminology for anatomical parts

The terminology and measurement of *Stegodon* tooth (see Figure 4) were modified from van den Bergh (1999).

The plate formula used:

x*N*x

x before the number *N* = the anterior cingulum.

N = total number of plates.

x after the number *N* = the posterior cingulum.

MicroCT scanning

Given that PRK_SC_P.01 is a deciduous tooth and potentially fragile, special care has been taken

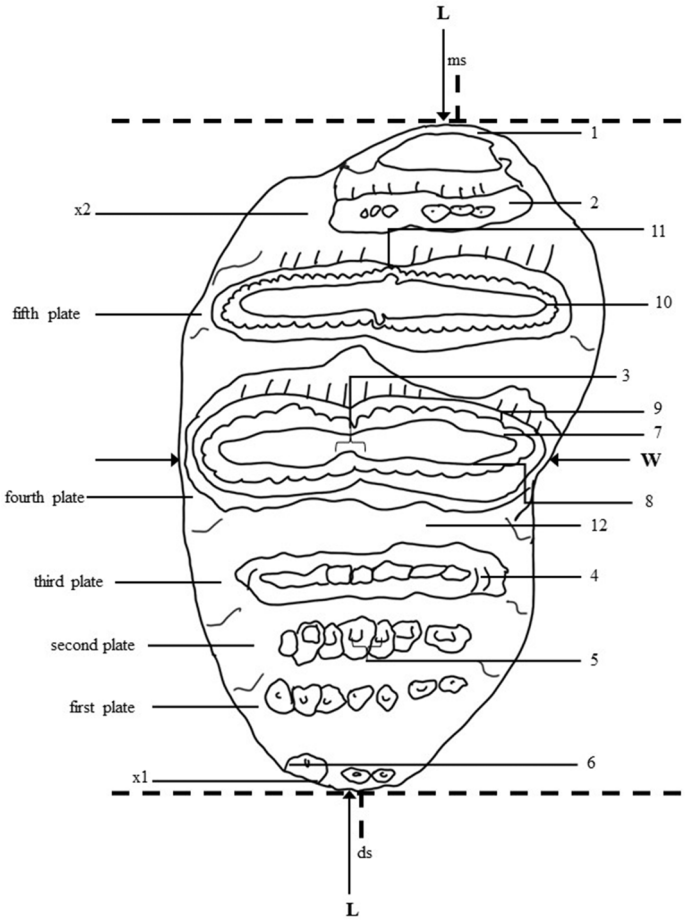

FIGURE 4. Terminology and biometric parameters used to describe *Stegodon* maxillary dp3 (occlusal view). ms = mesial, ds = distal, x1 = posterior cingulum, x2 = anterior cingulum, L = maximum length, W = maximum width, 1 = contact facet with preceding tooth, 2 = anterior plate, 3 = double median expansions of the enamel loop, 4 = enamel layer, 5 = enamel islands, 6 = conelet, 7 = complete enamel band with enamel wrinkles, 8 = inner enamel layer , 9 = outer enamel layer, 10 = dentine, 11 = transverse valley between plates, red dash line = median sulcus. Modified from van den Berg (1999).

during its preparation. The specimen is partially embedded in hard carbonate cave breccia, which bubbles under an acid test and reveals only about half of the specimen. Based on previous fossil extraction experience, where a heavy-duty battery-operated drill was used, it was determined that the breccia is too indurated for routine airbrushing techniques. The standard practice of soaking the sediment in acid to loosen it was also avoided due to concerns about damaging the delicate tooth. The use of micro-CT (μCT) technology significantly advances palaeontology by reducing the time and effort required for cleaning, especially with fragile specimens like this one.

The scanning was conducted at the scanning facility of the Universiti Malaya, using a Zeiss Xradia Versa 520 machine with a nanofocus transmission tube and moveable detector. The voxel size of the reconstructed volume is 63 μm in three dimensions. 3D rendering, meshes and movies were made using 3DSlicer software (Kikinis et al., 2014). Variations in the material density are visible through changes of greyscale from dark (low density, low attenuation) to light (high density, high attenuation). Segmentation of the volume was achieved with a combination of threshold and manual paint methods. Using the virtually isolated specimen, a set of measurements could be confidently obtained from the images.

pIR-IRSL dating of feldspars. A block sample of the surrounding breccia matrix was sampled in-situ using subdued red lights in dark cave conditions and wrapped in black plastic (Figure 3). Within subdued red-light conditions, the light-exposed outer layer was removed using a chisel and hammer and was retained as the dosimetry sample. These lay-

ers were broken up using a pestle and mortar and oven dried, then the entire fraction was milled and used for environmental dose estimation. The unexposed inner core was also gently broken up using a small hammer and was processed using the standard sample purification procedures for feldspar separation (Aitken, 1998) including a 10% wash in hydrofluoric acid for 10 minutes to remove the external alpha-dosed rinds (Rizal et al., 2020). All luminescence analysis was conducted at the 'Traps' luminescence dating facility at Macquarie University in Sydney, Australia.

To obtain an estimate of the environmental dose rate for each of the samples, we first measured beta dose rates using a Geiger-Muller multicounter beta counting of dried and powdered sediment samples (Botter-Jensen and Mejdahl, 1988) in the laboratory. Allowance was made for the effect of sample moisture content, different grain sizes (Brennan, 2003) and HF etching on attenuation of the beta dose, and the total beta dose-rate contribution was calculated by comparing the beta count rate to a standard beta source (SHAP with a dose rate of 5.99 Gy/kyr) and magnesium oxide as a non-beta emitting background material. Secondly, thick source alpha counting using a Daybreak 583 intelligent alpha counter was used to obtain estimates of Uranium and Thorium (Wang and Xia, 1991) to estimate the gamma dose rate, and thirdly the difference between beta and alpha counting was used to estimate potassium values. These estimates were then converted to gamma dose rates using the conversion factors of Guerin et al. (2011). Allowance was made for the effect of sample moisture content (Aitken, 1988) on the external beta and gamma dose rates using a long-term water content of between 2 ± 0.2 %, which is similar to the measured (field) water content of between 2.2% and allows for an initial period of saturation when first deposited in the karst environment.

The total dose rate was then calculated using an effective internal beta dose rate of 0.84 Gy kyr-1 (Huntley and Baril, 1997; Huntley and Hancock, 2001) for the 180-212 µm feldspar samples (due to the radioactive decay of 40K and 87Rb), which were made assuming K (12.5 ± 0.5%) and 87Rb (400 ± 100 µg g–1) concentrations and included in the total dose rate. Cosmic-ray dose rates were estimated from published relationships (Prescott and Hutton, 1994), making allowance for the thickness of limestone above the cave (~10 m with an assumed density of 1.2 g/cm^3), sediment overburden at the sample locality (1.0 m with an assumed density of 2.0 g/cm^3), the altitude (~20 m above sea level) and geographic latitude and longitude (4°S and 101°E) of the sampling site.

We used the 90-180 µm size fraction and stainless steel single aliquot discs for all the procedural tests using the following preheat and IR stimulation combinations: 1) 250 and 225°C (pIR-IRSL50,225)28,29; 2) 280 and 250°C (pIR-IRSL50,250)30; 3) 300 and 270°C (pIR-IRSL50,270)30; 4) 320 and 290°C (pIR-IRSL50,290)31,32; and as the expected De is >450 Gy, we also tested 5) 320 and 200/290°C (pIR-IRSL200.290)33. All tests followed these procedures 1) Preheat plateau and dose recovery tests - different preheat/IR laser stimulation combination was applied to each disc then a surrogate dose of 20 Gy was recovered, 2) Bleaching tests - a dose of 20 Gy was applied and bleached in a solar simulator for 4 hrs 3) Fading tests - testing anomalous fading in single-aliquots of feldspars.

The tests revealed that the flattest plateau was provided by the pIR-IRSL50,270, pIR-IRSL50,290 and pIR-IRSL200,290 signals, while the pIR-IRSL50,250 signal provided the best recovery of the surrogate dose (with a dose recovery ratio of 0.995) and lowest residual values after bleaching (<10 Gy) (although calculated, these residual doses were not subtracted from the De). Thus, the pIR-IRSL50,250 was chosen as the most suitable procedure for this sample with a fading correction of 1.7 % applied.

Single aliquots of potassium feldspar were processed first to gauge suitability for a subsequent single grain approach. Thus, single aliquot discs loaded with 90-125 µm feldspar grains were loaded onto a carousel and processed in a Riso TL-DA-20 containing an automated Detection and Stimulation Head (DASH) set up with a Dual laser single grain attachment with a Blue/UV sensitive Electron Tube PMT (PDM9107Q-AP-TTL-03) with maximum detection efficiency between 200 and 400 nm. The filters in the automated detection changer were set on the blue filter pack (Schott BG-39 and Corning 7-59 filters to transmit wavelengths of 320–480 nm (Hutt et al., 1988). The grains were stimulated using IR (830 nm) diodes for 250 s with the first 15 s as the signal and last the 100 s as background.

In addition, 180-212 µm feldspar grains were also processed but using aluminium single grain discs. They were loaded in the same reader with the same filter combination, but this time stimulated using a 830 nm 140 mW TTL modulated IR laser for 2.5 s, first at 50 °C and secondly at 270 °C

after a 300°C preheat according to the procedures of the pIR-IRSL protocol selected. The signal was integrated over the first 0.21-0.46 s with the last 1.88-2.5 s used as a background, with a standard exponential fit and monte carlo simulation for error determination.

U-series dating. We collected in situ flowstone stratigraphically above and below the *Stegodon* (Figure 3), which offers an opportunity to apply U–Th dating to bracket the *Stegodon's* age. Back in the lab, we carefully identified and selected the best calcite crystals, then cleaned them using ultrasonication with pure water. Procedures for U and Th chemical separation and purification are similar to those described in Edwards et al. (1987) and Shen et al. (2002). In short, calcite grains were dissolved in 7N nitric acid, mixed with an appropriate amount of ^{229}Th–^{233}U–^{236}U triple spike and dissolved iron. Then, ammonium hydroxide was added dropwise to increase the solution's pH until the appearance of iron oxyhydroxide precipitation. After removing the major Ca^{2+} ions with three times of centrifuging, the AG1-X8 resin (Bio-Rad) is used to separate and purify U/Th. All the chemical steps were performed on laminar-flow benches in a calss-1000 cleanroom. Uranium and thorium isotopic compositions were measured on a multi-collector inductively coupled plasma mass spectrometer (MC-ICP-MS), Thermo Scientific NEPTUNE, housed at the Department of Geosciences, National Taiwan University (Shen et al., 2012). Decay constants of 9.1705×10^{-6} yr^{-1} for ^{230}Th, 2.8221×10^{-6} yr^{-1} for ^{234}U (Cheng et al., 2013) and 1.55125×10^{-6} yr^{-1} for ^{238}U (Jaffey et al., 1971) were adopted. Age (relative to 1950 CE) was corrected using an initial $^{230}Th/^{232}Th$ atomic ratio of $4 \pm 2 \times 10^{-6}$. The uncertainties from all the sources were propagated through the U–Th age calculation and presented at the 2σ level or two standard deviations of the mean ($2\sigma_m$) unless otherwise noted. The detailed off-line data deduction and ^{230}Th date calculation were described in Shen et al. (2002). We tried two subsamples individually from above and below the *Stegodon*, in total four.

SYSTEMATIC PALAEONTOLOGY

Order PROBOSCIDEA Illiger, 1811
Suborder ELEPHANTIFORMES Tassy, 1988
Superfamily ELEPHANTOIDEA Osborn, 1921
Family STEGODONTIDAE Osborn, 1918
Genus STEGODON Falconer and Cautley, 1847

Stegodon sp.
Figures 5, 6

PRK_SC_P.01. A cheek tooth embedded in a conglomerate matrix.

Morphological descriptions

Peninsular Malaysia *Stegodon* (PRK_SC_P.01). The plate formula was determined to be x6x. Both the anterior and posterior cingula are preserved which indicate that this is a complete dp3 (see Figure 5). The tooth is brachydont and all the plates are unworn. From the exposed lateral view, the crown is longitudinally convex, the plates diverge apically, and constriction on the mesial end indicates that this is an upper tooth. The lateral convergence of plates suggested that the exposed side is lingual. All these characters show that this specimen is a left maxillary tooth.

In occlusal view, the posterior outline is broader compared to the anterior outline of the specimen. Each plate consists of cusps that are called 'conelets' and separated by longitudinal grooves. The median sulcus is well-developed in at least the anterior plates of the molar and does not reach the crown base. This median sulcus is prominent along the first to the third plates of the mesial end which divided the postrite and pretrite halves of the specimen. The mesial constriction is well-developed between the second and third plates of the mesial end. The lingual part is concave and the buccal end slightly convex in shape (see Figure 5).

In lingual view, the plates are bulbous towards the direction of the root, taper and thin towards the apex and take the shape of "roof". The valleys that separate the plates are Y-shaped, and the spacing of the plates increases anteriorly. Three plates at one end of the tooth are arranged more vertically which indicates that this is the posterior end of the tooth; the rest of the plates lean and converging apically which indicate that this is the anterior end of the tooth. The crown is higher towards the midline compared to the posterior and anterior ends. Both cingula are closely attached to the respective first plate at the anterior and the posterior ends of the tooth. There are no observable roots from this specimen (see Figure 6E), a fact which indicates that the roots were either not well developed or not preserved. The posterior cingulum consists of an estimated seven conelets. The first plate from the posterior end contains an estimated eight conelets. The penultimate and third plate (both from the posterior end) consist of an estimated eight and seven conelets, respectively. The fourth and fifth plate (both from the posterior end) both consist of five

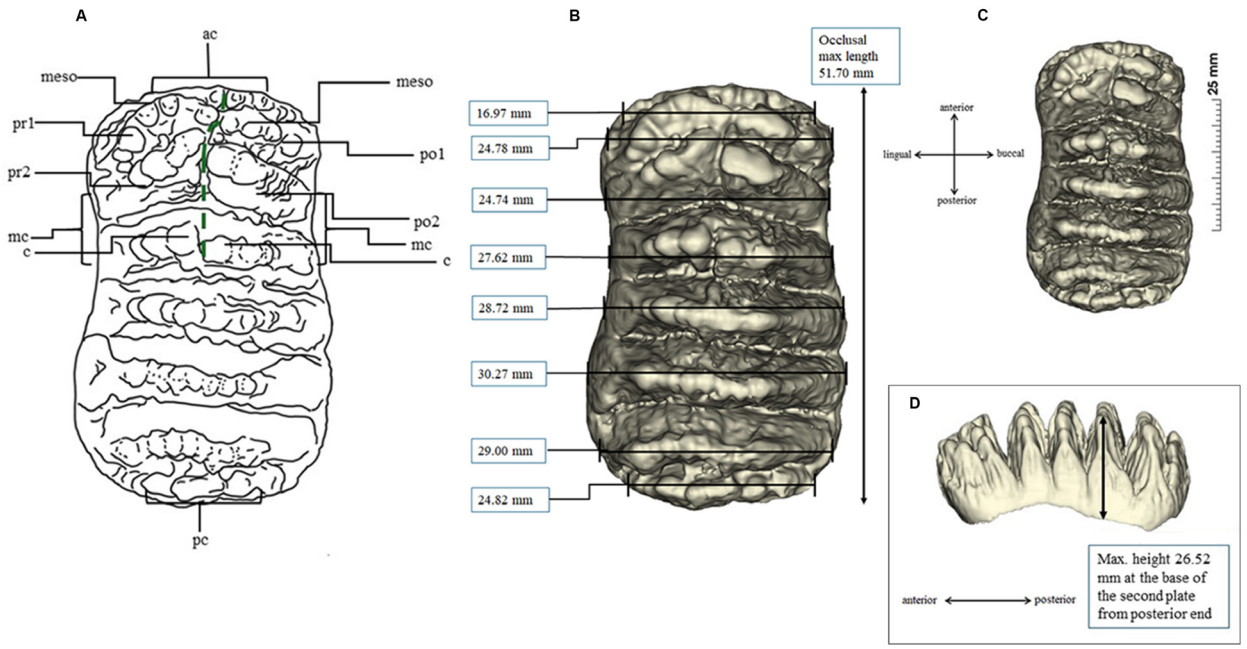

FIGURE 5. Fossil dp3 of *Stegodon* sp. from Gopeng, Perak (PRK_SC_P.01). A: Occlusal surface morphology based on µCT scanning. Key: ac, anterior cingulum; pc, posterior cingulum; meso, mesoconelet; pr1 and pr2, pretrite cusp of first and second plates from anterior end; po1 and po2, postrite cusp of first and second plates from mesial end; c, conelets; mc, mesial constriction; green dash line, median sulcus, B: measurement of lingual-buccal of each plate (in mm), C: occlusal view, and D: lingual view.

conelets. The sixth plate from the posterior end has an estimated nine conelets and contains an anterior cingulum. This anterior cingulum consists of an estimated six conelets and is fused with the first plate of the mesial end towards the middle.

Comparison materials

***S. orientalis* (KL DP3).** The plate formula was determined to be x5x, and the crown is brachydont. The posterior end is complete with smooth texture while the anterior end is incomplete, judging from the hard texture and abrasion seen at this end. This tooth is slightly used, the first three plates from the posterior end and posterior cingulum are not used. However, the fifth plate from the posterior end is heavily used with a single large enamel island and exposed dentine. The median sulcus that separates the postrite and pretrite halves is most observable at the third and fourth plates from the posterior end. From the sagittal section, the crown is longitudinally convex, and the plates diverge apically, and there is a constriction on the mesial end which indicates that this is an upper cheek tooth. All these characters show that this specimen is a tooth from the right maxilla.

From the lateral view, the plates are bulbous towards direction of the root, taper and thin towards the apex and “roof” shaped (see Figure 7). The valleys that separate the plates are Y-shaped, and the spacing of the plates increases anteriorly. Two plates at one end of the tooth are arranged more vertically which indicates that this is the posterior end of the tooth; the rest of the plates leaning and converging apically which indicate that this is the anterior end of the tooth. The crown is higher towards the posterior end compared to the anterior. The buccal side of the anterior cingulum is damaged and only the lingual side of the anterior cingulum can be observed from this specimen. There are no observable roots from this specimen which indicates that the roots were either not well developed or not preserved.

The posterior cingulum has nine unworn conelets. The first, second and third plates (all from the posterior end) have an estimated 14, 11 and 12 conelets, respectively, all not in use. Mesoconelets between the sixth and seventh conelets from the lingual side can be observed from the posterior end. The fourth plate from the posterior end shows the division of the postrite and pretrite sides, where the lingual side is slightly used, and the conelets are fused together to form one single large enamel island. The fifth plate from the posterior end has

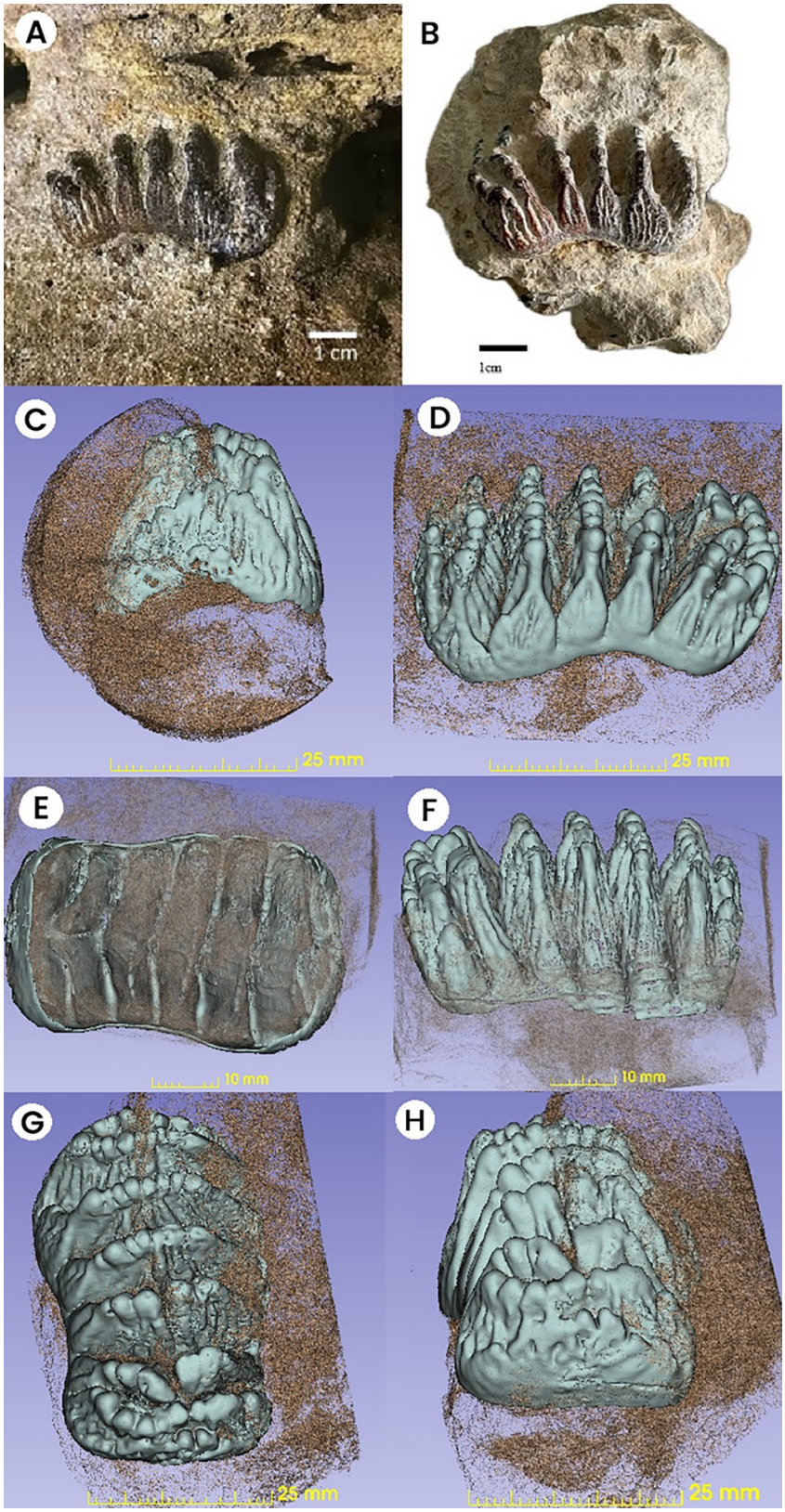

FIGURE 6. In situ and high-throughput µCT images of PRK_SC_P.01. A: lingual view, embedded in cave breccia before extraction. B: lingual view, after extraction but still embedded in matrix. C: the mesial end. D: lingual side in mirror image. E: the underneath view. F: buccal view in mirror image. G: occlusal view, and H: the distal end.

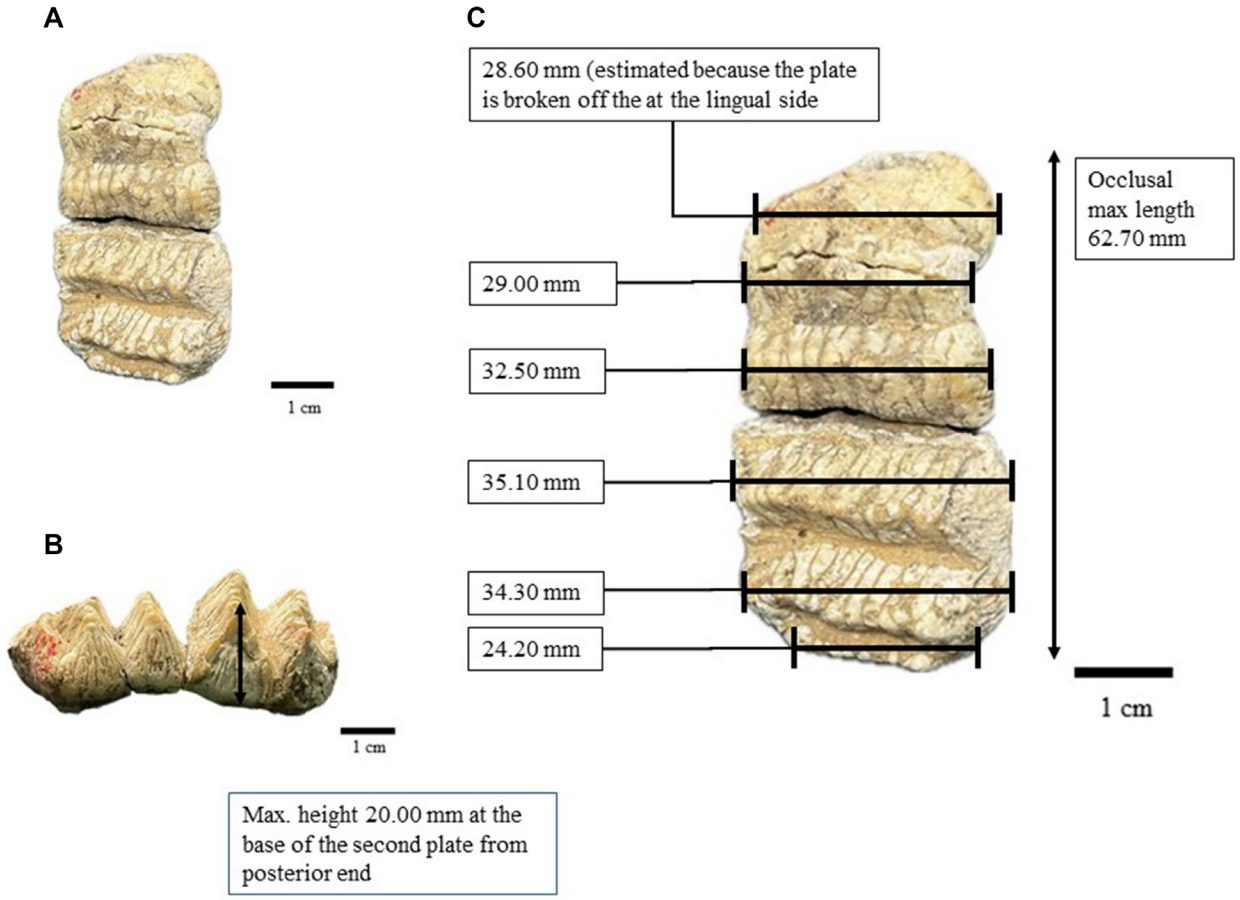

FIGURE 7. Fossil dp3 of *Stegodon orientalis* (KL DP3) from Keo Leng Cave in northern Vietnam. A: occlusal view, B: buccal view, and C: width measurement of lingual-buccal of each plate (in mm).

enamel fused to form one single large enamel island. The anterior cingulum is not fully preserved.

The tooth is more convex at the posterior end, tapered at the anterior end at the third plate from the posterior end (mesial constriction) and convex again at the anterior end.

***S. trigonocephalus* (CD 11649).** The plate formula of this specimen was determined to be (+)5(+)x. The posterior end of the specimen is complete, but it is damaged at the mesial-lingual side (see Figure 8). The specimen is a slightly worn left upper dp3. The first two plates from the posterior end have a high number of conelets (10 or more) compared to the subsequent plates (which have less than 10 conelets). These two plates are not in use. Formation of small enamel islands (digitation) can be seen at the third and fourth plates from the posterior end and larger enamel islands can be seen at the lingual side of the fifth plate from the posterior end. Enamel wrinkles are most obvious at the fourth and fifth plates from the posterior end. A prominent median sulcus which divides the postrite and pretrite halves can be observed towards the posterior end. An obvious subdivision in two parts can be seen at the second plate from the posterior end, of which the lingual side is wider than the buccal side.

From the sagittal section, the crown is longitudinally convex, the plates diverge apically, and there is constriction on the mesial end which indicates that this is an upper cheek tooth. All these characters show that this specimen is a tooth from the left maxilla.

From the lateral view, the plates are bulbous towards direction of the root, taper and thinner towards the apex, and “roof” shaped. The valleys that separate the plates are Y-shaped, and the spacing of the plates increases anteriorly. Three plates at one end of the tooth are arranged more vertically which indicates that this is the posterior end of the tooth; the rest of the plates lean and converge apically which indicates that this is the

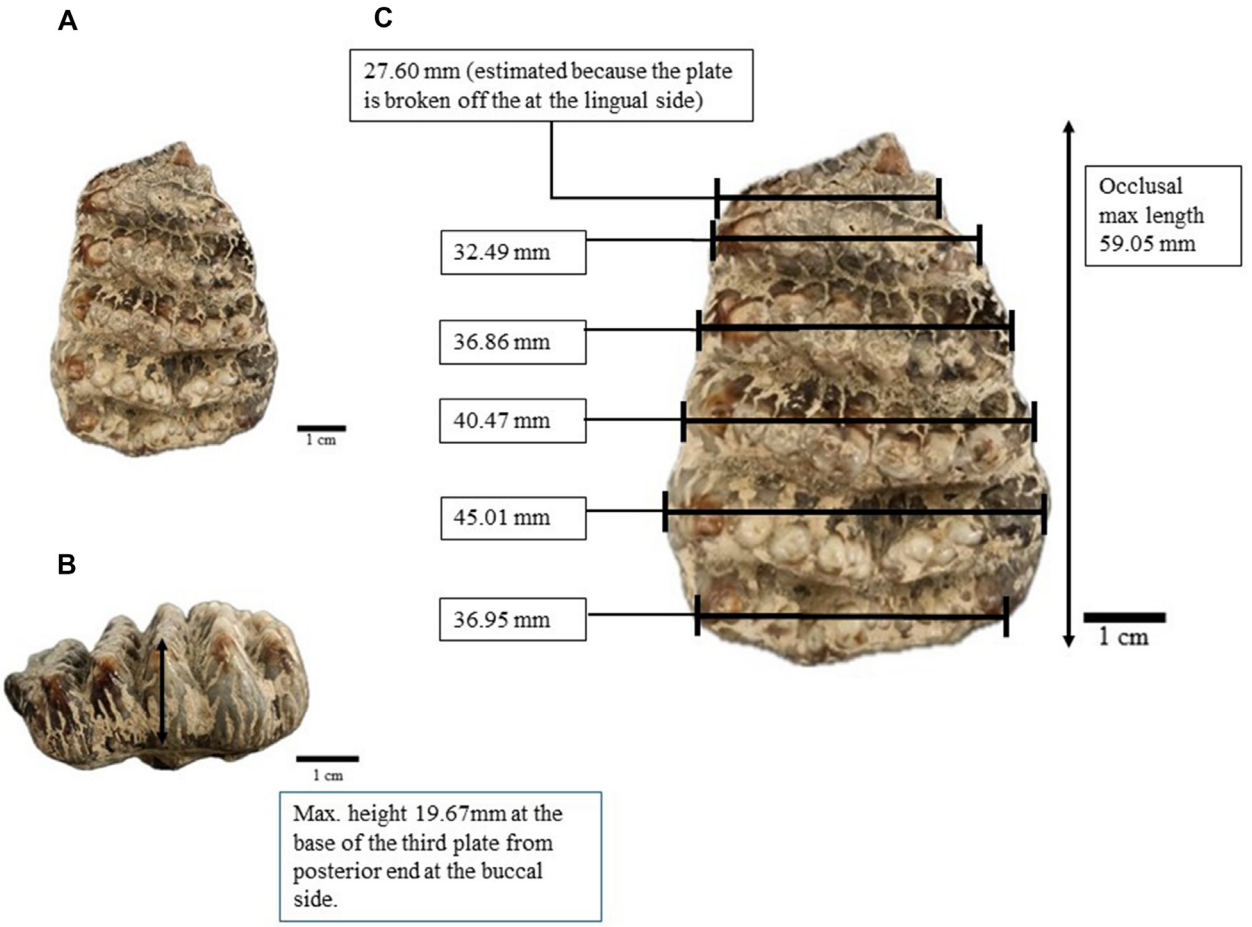

FIGURE 8. Fossil dp3 of *Stegodon trigonocephalus* (CD 11649) from Java, Indonesia: A: occlusal view, B: buccal view, and C: width measurement of lingual-buccal of each plate (in mm).

anterior end of the tooth. The crown is higher at the second and third plates from the posterior end. It is difficult to determine if the cingulum is present as the anterior end is broken. However, a cingulum is observed fully attached to the first plate from the posterior end. There are no observable roots from this specimen. Plate dimensions of all three specimens are summarized in Table 2.

Geochronology

The pIR-IRSL dating of the breccia matrix constrained the tooth to 233 ± 31 ka according to 12 single aliquots of feldspar and 199 ± 28 ka based on 116 single grains of feldspars. These results are coeval with error margins and reflect the difference in approaches between the aliquots and single grains methods. Due to the large number of grains on single aliquot discs an averaging effect occurs on the luminescence signal. Thus, the single aliquot result due to its opportunity to observe partially bleached grains is usually slightly younger and more reliable for age determination.

Only one age was obtained (see Table 3) from the U-series dated sample, since the other ones contain too much detritus to give any reasonable results. The concentrations of ^{238}U and ^{232}Th in the sample are ~171 ppb and ~114 ppb respectively. The yield age is 35184 ± 9485 yr BP.

The combined in-situ sediment dating of the breccia matrix and overlying flowstone reveal that the fossil was deposited in this location before 35 ± 10 ka (U-series dating of flowstone, see Table 3) and between 171-264 ka (233 ± 31-199 ± 28 ka) (pIR-IRSL dating of feldspars, see Table 4) with examples of the pIR-IRSL dating of feldspars data presented in Figure 9. The two dating results agree with each other and are consistent with their stratigraphic location. Due to the error margin associated with the pIR-IRSL age estimate there is a good chance that the *Stegodon* individual died

TABLE 2. Plate dimensions (in mm) of PRK_SC_P.01, *S. trigonocephalus* (CD 11649), and *S. orientalis (*KL DP3). **TL**: total length; **MH**: maximum height; **LF**: lamellar frequency; **H/W**: Height/Width Index.

Specimen / Dimension		PRK_SC_P.01	CD 11649	KL DP3
Width of each plate (mm)	x (posterior)	24.82	-	24.20
	1st	29.00	36.95	34.30
	2nd	30.27	45.01	35.10
	3rd	28.72	40.47	32.50
	4th	27.62	36.86	29.00
	5th	24.74	32.49	28.60 (estimated)
	6th	24.78	27.60 (estimated)	-
	x (anterior)	16.97	-	-
TL (mm)		51.70	59.05	62.70
MH (mm)		26.52 (taken at the 2nd plate from the posterior end)	19.67 (taken at the 3rd plate from the posterior end)	20.00 (taken at the 2nd plate from the posterior end)
LF		11.61	10.16	7.97
H/W Index		87.61	43.70	56.98

TABLE 3. Uranium and Thorium isotopic compositions and ^{230}Th age by MC-ICP-MS at NTU.
Analytical errors are 2σ of the mean.

Chem ID	^{238}U (10^{-9}g/g [a])	^{232}Th (10^{-9}g/g)	δ^{234}U measured [a]	[^{230}Th/^{238}U] activity [c]	^{230}Th/^{232}Th atomic (x 10^{-6})
210107-A2-U	171.12 ± 0.12	114.5 ± 1.5	50.2 ± 1.9	0.4083 ± 0.0023	10.06 ± 0.14

Age (yr ago) uncorrected	Age (yr ago) corrected [c, d]	Age (yr BP) relative to 1950 CE	$\delta^{234}U_{initial}$ corrected [b]
53,436 ± 415	35,255 ± 9945	35,188 ± 9945	55.4 ± 2.6

[a] $[^{238}U] = [^{235}U] \times 137.77$ (±0.11‰) (Hiess et al., 2012); $\delta^{234}U = ([^{234}U/^{238}U]_{activity} - 1) \times 1000$.

[b] $\delta^{234}U_{initial}$ corrected was calculated based on ^{230}Th age (T), i.e., $\delta^{234}U_{initial} = \delta^{234}U_{measured} \times e^{\lambda 234 * T}$, and T is corrected age.

[c] $[^{230}Th/^{238}U]_{activity} = 1 - e^{-\lambda 230 T} + (\delta^{234}U_{measured}/1000)[\lambda_{230}/(\lambda_{230} - \lambda_{234})](1 - e^{-(\lambda 230 - \lambda 234) T})$, where T is the age.
Decay constants are 9.1705 x 10^{-6} yr^{-1} for ^{230}Th, 2.8221 x 10^{-6} yr^{-1} for ^{234}U (Cheng et al., 2013), and 1.55125 x 10^{-10} yr^{-1} for ^{238}U (Jaffey et al., 1971).

[d] Age corrections, relative to chemistry date in January 2021, were calculated using an estimated atomic ^{230}Th/^{232}Th ratio of 4 (± 2) x 10^{-6}.

within this age range and was later deposited within the cave breccia.

DISCUSSION

PRK_SC_P.01 remains the only and most well-preserved *Stegodon* specimen from Peninsular Malaysia. The discovery of the *Stegodon* fossil here is a testimony to the wide distribution range of this genus during middle Pleistocene time in the Sundaic subregion. Even though large parts of the tooth are still embedded in matrix, the use of micro-CT is helpful in revealing the full morphology of the specimen for comparison to be made with related middle Pleistocene non-dwarf species of *Stegodon* found in the Sundaic subregion (Table 1). The age range for this individual based on the pIR-IRSL and

TABLE 4. pIR-IRSL coarse grain dating of sediments at *Stegodon* Cave: dose rate data, equivalent doses, and age estimates.

Sample code[a]	MAL-STEG	
Depth (m)[b]	1.0	1.0
Gamma dose rate (Gy ka^{-1})[c]	1.590 ± 0.196	1.590 ± 0.196
Beta dose rate (Gy ka^{-1})[c]	1.605 ± 0.051	1.518 ± 0.049
Cosmic-ray dose rate (Gy ka^{-1})[d]	0.085 ± 0.002	0.085 ± 0.002
Internal dose rate (Gy ka^{-1})[e]	0.72 ± 0.10	0.84 ± 0.20
Water content (%)[f]	2 / 2 ± 0.2	2 / 2 ± 0.2
Total dose rate (Gy ka^{-1})	4.00 ± 0.26	4.03 ± 0.32
Accepted /Run aliquots[g]	11/12	116/500
Technique[h]	**pIR-IRSL$_{SA}$**	**pIR-IRSL$_{SG}$**
Equivalent dose (Gy)[i,j]	932 ± 104	801 ± 94
Age (ka)[j]	**233 ± 31**	**199 ± 28**

[a] Samples processed using the 90-125 (SA) and 180-212 (SG) µm size fractions.

[b] Samples heights were measured against the upper flowstone at the site

[c] Beta dose rates were estimated using a Geiger Muller beta counting of dried and powdered sediment samples, gamma dose rates were estimated using an insitu gamma spectrometer and tested against thick source alpha counting measurements of dried and powdered sediment samples in the laboratory. The difference between the alpha and beta measurements was used to estimate potassium values.

[d] Time-averaged cosmic-ray dose rates (for dry samples), each assigned an uncertainty of ± 10%.

[e] Mean ± total (1σ) uncertainty, calculated as the quadratic sum of the random and systematic uncertainties.

[f] Field / time-averaged water contents, expressed as (mass of water/mass of dry sample) x 100. The latter values were used to correct the external gamma and beta dose rates.

[g] Total number of aliquots/grains processed verses number of accepted aliquots/grains- with an average acceptance rate of ~90%

[h] pIR-IRSL$_{SA}$ indicates coarse grain feldspars using 90-125 µm grains, pIR-IRSL$_{SG}$ indicates coarse grained feldspars using 180-212 µm grains

[i] Equivalent doses include a ± 2% systematic uncertainty associated with laboratory beta-source calibrations, and represents a fading corrected D_e. Fading corrections according to Lamothe et al. (2003)

[j] Uncertainties at 68% confidence interval.

U-series chronology lies within the expected age range for *Stegodon* found on mainland Southeast Asia.

Differences and similarities between PRK_SC_P.01 *(Stegodon* sp.) and the dp3s of *S. trigonocephalus* and *S. orientalis*

The posterior cingulum of KL DP3 is only very low and weakly developed, while in PRK_SC_P.01 and the *S. trigonocephalus* specimen examined, the posterior cingulum almost resembles all the other true plates. However, this might be due to individual variation in the development of these terminal plates or talons. KL DP3 may resemble some specimens from mainland China in having five ridges and a small talon (posterior cingulum), but PRK_SC_P.01 and CD 11649 seem to resemble the condition reported for some dp4 specimens from Yenchingkou and Paxian Dadong, in which the cingulum is so well developed that it can be considered as a fully developed plate (e.g., A.M.N.H. no. 18705, described in Osborn, 1942; Colbert and Hooijer, 1953; Schepartz et al., 2005). However, the anterior or posterior cingulum in these Chinese dp4 specimens do not seem to have any associated row of small enamel tubercles as is in PRK_SC_P.01.

The enamel tubercles on the apical of the plates in PRK_SC_P.01 are larger as compared to those of *S. trigonocephalus* but these tubercles are smaller and less developed in the *S. orientalis* specimen examined. Towards the lower end of the enamel tubercles, the plates of PRK_SC_P.01 are highly tapered, less so in the *S. trigonocephalus*

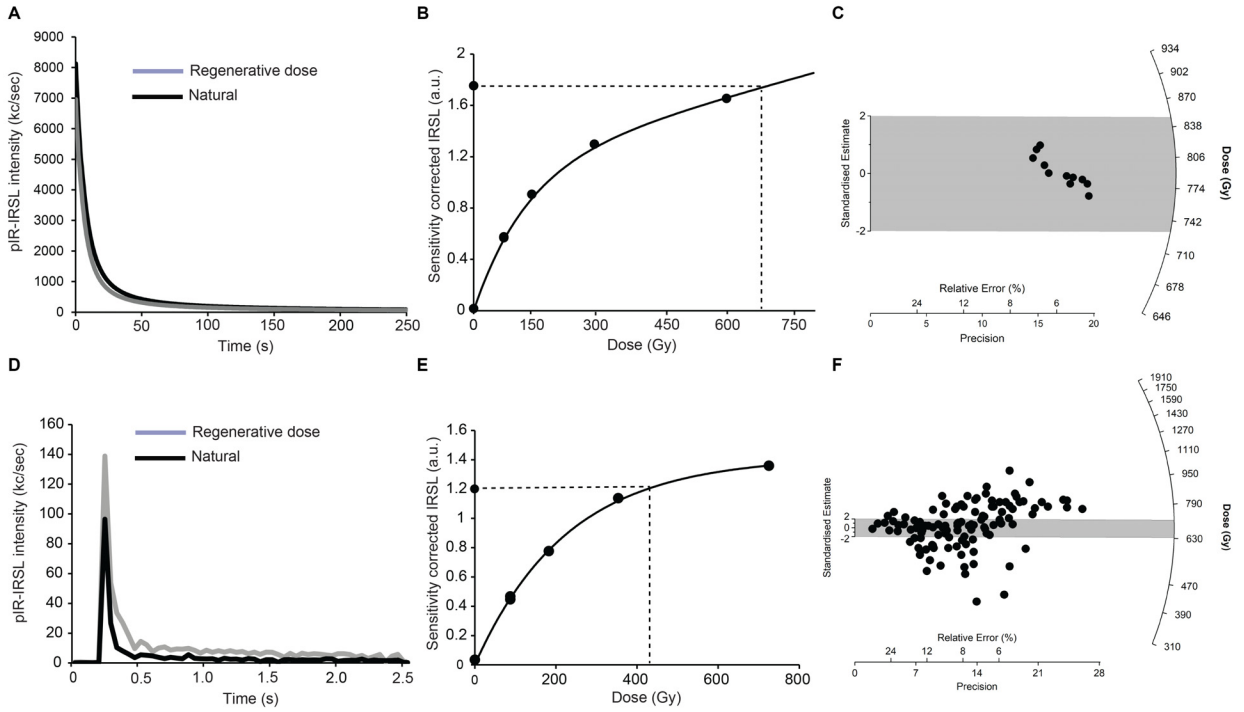

FIGURE 9. The resulting pIR-IRSL data from aliquots and grains of feldspars from the breccia matrix in the *Stegodon* Cave. A: shine down curve for single aliquot data including both the natural and regenerative dose, B: the dose response of the sample aliquot with a De of 675 ± 18 Gy, a recycling ratio of 1.04 ± 0.03 and a D0 of 1136 ± 139 Gy, C: the corresponding radial plot for this sample with an uncorrected CAM of 757 ± 34 Gy (n=12 aliquots), D: shine down curve for single grain data including both the natural and regenerative dose, E: the dose response of the single grain with a De of 422 ± 12 Gy, F: the corresponding radial plot for this sample with an uncorrected CAM of 679 ± 26 Gy (n=116 grains).

and *S. orientalis* specimens. PRK_SC_P.01 conelets are smaller and less bulbous compared to those of *S. orientalis*. From lingual view, PRK_SC_P.01 has gracile plates and higher crowns as compared to the *S. trigonocephalus* and *S. orientalis* specimens. The valley between the plates of PRK_SC_P.01 is shallower compared to both *S. trigonocephalus* and *S. orientalis.* These features are summarized in Table 5 and Figure 10.

PRK_SC_P.01 shared some of the common morphological features with *S. trigonocephalus* and *S. orientalis* – greater number of plates than those of primitive *Stegodon* species such as *S. zdanskyi*, widely spaced ridges, vertical grooves along the lingual and buccal surfaces, and relatively low crowned. However, metrical analysis shows that PRK_SC_P.01 has different parameters and measurements from these two species. PRK_SC_P.01 has high lamellar frequency values

TABLE 5. Summary of the characteristic differences between the dp3s of PRK_SC_P.01, *S. orientalis* (KL DP3), and *S. trigonocephalus* (CD 11649).

No.	Characters	PRK_SC_P.01	*S. orientalis*	*S. trigonocephalus*
1.	Development of posterior cingulum	Moderately developed	Weakly developed	Developed
2.	Presence of enamel tubercules at posterior cingulum	Present	Absent	Present
3.	Tapering of each plate	High	Minimal	Moderate
4.	Thickness of plate	Thin	Thick	Thick
5.	Depth of valley between plates	Low	High	High

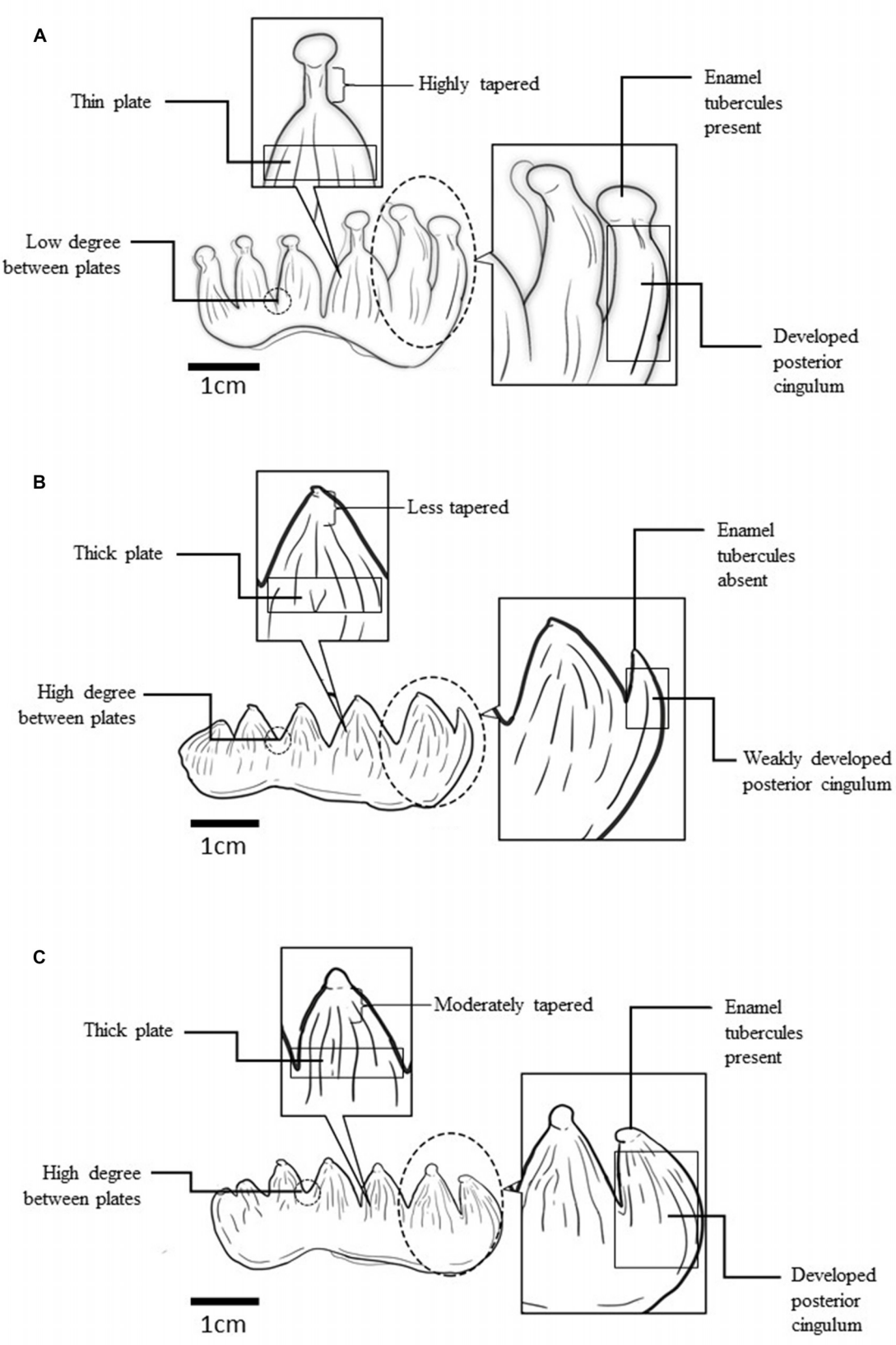

FIGURE 10. Illustration showing morphological differences between the dp3s. A: PRK_SC_P.01, B: *S. orientalis*, KL DP3, C: *S. trigonocephalus*, CD 11649.

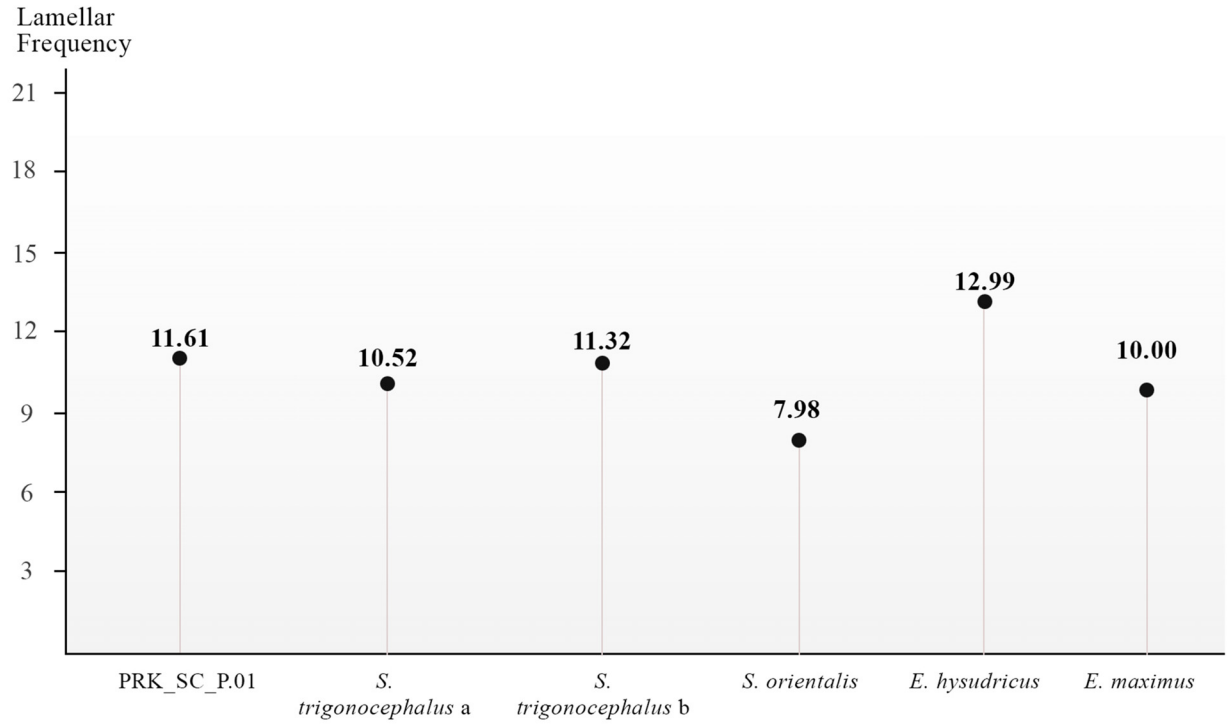

FIGURE 11. The lamellar frequency of dp3 from six different specimens. Four of the specimens from the genus *Stegodon*: PRK_SC_P.01 (*Stegodon* sp.); CD 11647a and CD 11647b from Java, Indonesia *(S. trigonocephalus);* KL DP3 from Keo Leng, Vietnam *(S. orientalis).* Values for the Asian elephant, *Elephas maximus* (ZRC 4.1669 LKCNHM) and *Elephas hysudricus* (CD 11702 from Java, Indonesia) was added for comparison. Source of data: CD 11647a and CD 11647b from Hooijer (1955).

(LF), 11.61 (Figure 11) which is quite different from the dp3 of *S. orientalis* (KL DP3) that has a relatively low value of 7.98. However, as compared to both *S. trigonocephalus* specimens from Java (CD 11647a and CD 11647b), PRK_SC_P.01 shows almost similar in terms of LF values as both Java specimens which have high LF, 10.52 and 11.32, respectively. As compared to the genus *Elephas,* PRK_SC_P.01 shows a higher value than the living Asian elephant *(E. maximus)* but lower than the extinct *E. hysudricus*.

From comparative morphological studies with other *Stegodon* specimens *(S. trigonocephalus* and *S. orientalis)* PRK_SC_P.01 differs in morphology from *S. orientalis* and less so from *S. trigonocephalus*. Due to this limitation and the observed morphological differences, it is currently not possible to assign a definite species to PRK_SC_P.01. Further comparisons with other *Stegodon* species both continental and island species are needed to address the exact taxonomic status of this specimen.

The lack of cementum from the µCT images of PRK_SC_P.01 might indicate that this layer is yet to be developed as it is still a milk tooth. The absence of cementum, a common occurrence in the early stages of tooth development in mammals, occurs because this layer is formed much later than the enamel and dentin layers (Foster, 2017). The cementum has a close anatomical relationship to the root dentine, which is not yet fully developed in PRK_SC_P.01 (see Figure 12).

Most of the continental *Stegodon* fossils that were discovered in middle to late Pleistocene of Southeast Asia were assigned either definitely or tentatively to the species *S. orientalis*, except for some examples discovered in a middle Pleistocene site in Tam Nang, Laos (Arambourg and Fromaget, 1938), which were identified as belonging to *S. sinensis*. According to Chen (1999), remains of *Stegodon* from southern China were mostly assigned to *S. orientalis*. Our results of morphological comparison indicated that PRK_SC_P.01 exhibits morphological characters that are different from *S. orientalis*. This implies that either the species is highly variable in the characters considered here (Table 5) or, alternatively, there might be a greater level of taxonomoic diversity of *Stegodon* in middle

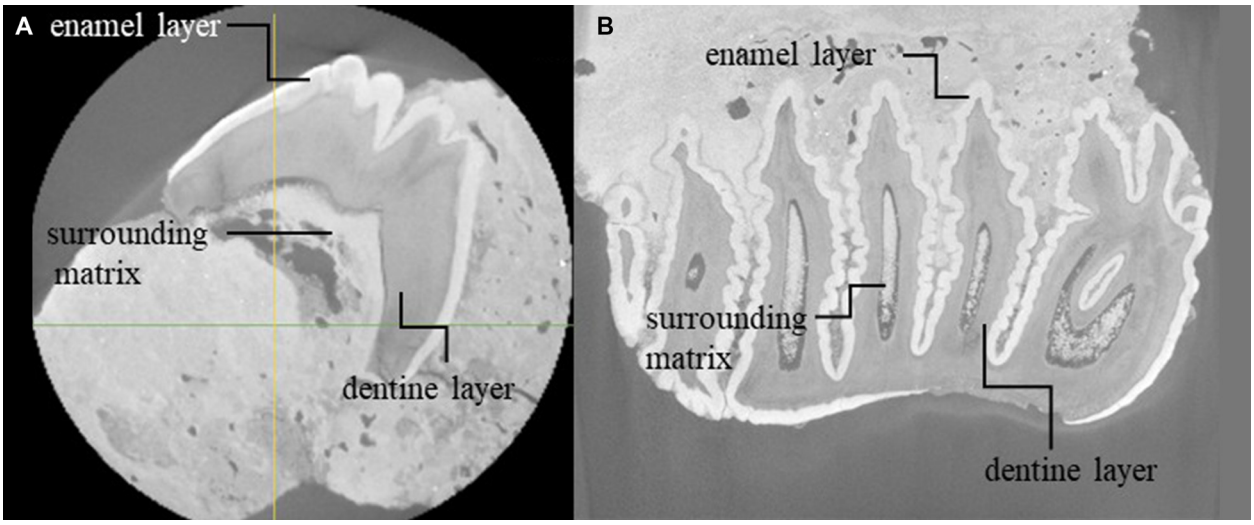

FIGURE 12. Cross-section µCT images of PRK_SC_P.01. A: mesial-distal view, B: occlusal–root view, showing the inner layers of the tooth and surrounding matrix.

to late Pleistocene continental Southeast Asia that has yet to be fully recognized.

Biogeographic implications

Stegodon remains have been found on mainland Southeast Asia, ranging in age from earlier Pleistocene, such as in the Irrawaddy beds, Myanmar (Colbert, 1943), to late Pleistocene deposits in Vietnam, Myanmar, and Laos (Olsen and Ciochon, 1990; Zin-Maung-Maung-Thein et al., 2011; Bacon et. al, 2018). The oldest documented evidence of *S. orientalis* comes from Dayakou, located in southwest China, while *S. trigonocephalus* was first recorded in Ci Saat, Java (Sondaar, 1984; van den Bergh et al., 2001a). These two species of *Stegodon* were, therefore, determined to have evolved during the earlier phase of Pleistocene period. As for the *Stegodon* from island Southeast Asia, their remains were found from early Pleistocene in Ci Saat up to the late Pleistocene deposits in Liang Bua (Flores) (van den Bergh et al., 2001a, 2008).The age range for PRK_SC_P.01 based on the pIR-IRSL and U-series chronology lies within the expected age range for *Stegodon* found on mainland Southeast Asia during the middle Pleistocene. The middle Pleistocene of the Tham Khuyen and Tham Hai in Vietnam, where *S. orientalis* specimens were discovered, indicate between roughly 300,000 to 200,000 years old based on the dating of biostratigraphic ground (Long and Du, 1981). Remains of *S. trigonocephalus* had also been reported from middle Pleistocene sites in Java, including Kedung Brubus (0.8 – 0.7 Ma, based on the faunal assemblages [van den Bergh et al., 2001b]), Ngandong (142 – 92 ka, according to thermoluminescence, pIR-IRSL, and $^{40}Ar/^{39}Ar$ methods [Rizal et al., 2020]), Trinil HK (0.54 ± 0.10 Ma – 0.43 ± 0.05 Ma, based on $^{40}Ar/^{39}Ar$, palaeomagnetic and luminescence dating method [Joordens et al., 2015]), and Trinil HK Bone Bearing Channel 2 (450 ± 110 ka – 430 ± 50 ka [Hilgen et al., 2023]).

The discovery of *Stegodon* sp. reported here represents the geologically youngest fossil evidence of *Stegodon* found in the Malay Peninsula, specifically in the southern region below the Kra Isthmus. This isthmus serves as a demarcation between the Indochinese and Sundaic subdivisions of the contemporary Southeast Asian zoogeographical regions (Corbet and Hill, 1992). PRK_SC_P.01 represents the southernmost *Stegodon* in continental Asia, situated amidst two prominent groups of *Stegodon.* Although the *Stegodon* specimen from Peninsular Malaysia exhibits distinct morphologies as compared to the other two main taxa, it is challenging to ascertain whether this specimen represents a transitional species between the continental and island forms of *Stegodon*. This difficulty arises due to the limited information and the singular nature of the *Stegodon* specimen from Peninsular Malaysia. PRK_SC_P.01 does not show any distinctive morphologies that can help to identify whether it is a continental or insular species from the Sundaland during the middle Pleistocene. Regardless, by comparing the size of PRK_SC_P.01 to both *S. orientalis* and *S. trigonocephalus* specimens, PRK_SC_P.01 does not exhibit any dwarfism in

size. PRK_SC_P.01 affirms that there were populations of this genus in the region, however, it remains unknown whether they were the direct descendants of either *S. orientalis* (continental species) or *S. trigonocephalus* (insular species), or from a transitional species as both of these species were found in early Pleistocene times.

Stegodon and palaeoenvironment

Dental microwear analysis of *S. orientalis* from southern China shows that the species was primarily browsers in a more densely forested landscape (Zhang et al., 2017). This is different from the *S. trigonocephalus* of Java which shows that the species was mostly grazers in an environment dominated by a mix of open savannah woodlands and evergreen forests (Puspannigrum et. al, 2020). Securely dated middle Pleistocene fossil sites from Peninsular Malaysia are few in number, but all have yielded mammalian remains from taxa that are known to have included forest environment as part of their natural habitats in modern times (Ibrahim et al., 2013). Indicative taxon frequently used for palaeoenvironmental reconstruction such as *Pongo* had been reported from all of these sites in Peninsular Malaysia (Ibrahim et al., 2013) and also from the *Stegodon* Cave (Muhammad et al., 2020). The presence of *Pongo* among fossil mammal assemblages was previously taken as a definite indication of an environment that was predominantly forest (Tougard, 1998; Storm et al., 2005). However, there is growing evidence from recent studies which showed that modern representatives of the genus can not only live in continuous closed-canopy rainforests but are also capable of surviving in altered landscapes dominated by secondary forests and farmlands (Wich et al., 2008; Oram, 2018; Sabah Wildlife Department, 2020; Ancrenaz et al., 2021), with some of the fossil *Pongo* exhibited isotopic signals indicating broader dietary spectrum and being discovered in drier environments from the end of the Last Interglacial until the late Holocene (Westaway et al., 2007; Louys et al., 2021, 2022). As a result, the presence of *Pongo* within the same stratum of PRK_SC_P.01 cannot now in itself be regarded as an unequivocal evidence of the predominant occurrence of closed-canopy tropical rainforests (to the exclusion of other similar environments) in the area during middle Pleistocene times. However, based on our current knowledge of the ecological tolerance of modern *Pongo* and isotopic evidence of fossil *Pongo* and *Stegodon* from elsewhere in Southeast Asia and adjacent areas, it is reasonable to suggest that the palaeoenvironment of the *Stegodon* Cave site during middle Pleistocene may have been either under continuous forest cover or a mixed landscape with patches of forests interspersed among more opened vegetation. Nevertheless, more comprehensive studies are needed to properly reconstruct the detailed palaeoenvironment in this region, since mammal assemblages that were discovered in *Stegodon* Cave were the results of upbringing from the stream that flows along the periphery of the cliff. Further analysis of the palaeoenvironment could enhance in identifying the correlation of PRK_SC_P.01 to the *S. orientalis* or *S. trigonocephalus*, or perhaps a species that transitions between the continental or islandic species.

CONCLUSIONS

The specimen PRK_SC_P.01 represents the only known record of *Stegodon* from Peninsular Malaysia. This late middle Pleistocene specimen shows a unique combination of characters as compared to two species of *Stegodon* found in the region, namely *S. orientalis* and *S. trigonocephalus*, which lived during the early to late Pleistocene. Characters unique to PRK_SC_P.01 include a strongly developed posterior cingulum as compared to *S. orientalis* from Vietnam, but slightly less developed than in *S. trigonocephalus* from Java. It also has enamel tubercles present at the posterior cingulum, and highly tapered plates at the lingual side of the tooth. As compared to both *S. orientalis* and *S. trigonocephalus,* the specimen from Peninsular Malaysia has thinner plates with shallower valleys between them. The discovery of *Stegodon* in Peninsular Malaysia indicates there were representatives of this genus in the region at least before 199 ± 28 and 233 ± 31 ka. It remains unclear whether this middle Pleistocene *Stegodon* represented the direct descendants of the continental species from the north or the insular species from the south.

ACKNOWLEDGEMENTS

This research was supported by GPF021B-2018: Studies On Middle–Late Pleistocene Vertebrate Teeth Fossils In Karst In Peninsular Malaysia and IIRG004A-2020FNW: Top Down: Evolutionary Dynamics Study Of Quaternary Faunal Remains From Karstic Landscapes Of Peninsular Malaysia, both provided by Universiti Malaya awarded to RFM. The luminescence dating aspects of the proj-

ect were funded by an ARC Discovery grant DP230100440 to KEW.

Our team would like to thank members of Kinta Valley Watch (KVW), especially B.T. Ching , C.Y. Tee, Y.L. Nang, J.C. Chan, and J.F. Chan who first discovered the fossil and reported to the authority. Appreciation goes to the 5th Earl of Cranbrook (G. Gathorne-Hardy), J. de Vos, G. van den Bergh, G. Drawhorn, C. Chang, P. Piper, A. Wattanapituksakul, S.Z.H. Wen, J. Ma, and J. Duangkrayom for their help with earlier identification of the specimen from Peninsular Malaysia. We sincerely acknowledge Dr. C.-C. Shen of the Department of Geosciences, National Taiwan University, for the approval of U-Th dating facilities. AHA expresses his gratitude to the Vietnam Institute of Archaeology (Hanoi) for the opportunity to examine their Stegodon fossils, to L.K. Chian Natural History Museum (LKCNHM, National University of Singapore) for the opportunity to examine their Elephas maximus specimen, to M. Tablizo, M. Puspaningrum, and H.Q. Le for their valuable insights concerning Stegodon in the Philippines, Indonesia and Vietnam, and to Z. Zahari for his assistance in arranging and formatting the figures in this manuscript. RFM is grateful to N.I. Taib for the help with the fossil 3D model printing, F.A. Zulkifli for helping with the GIS, F.M. Razif and Z. Kem who kindly helped in the field and to M.N.A. Rahman, N.A. Md Nur from the Department of Mineral and Geoscience Malaysia for research permission and S.R. Hussein and A.M. Yazrol from the Perak State Parks Corporation for facilitating the fossil extraction. LTT would like to thank Vereniging Nederland-Maleisië (VNM) for a research grant to the Netherlands, Naturalis Biodiversity Center for permission to study their *Stegodon* collection, and to H. van de Bunte, N. den Ouden, and A. van Westbroek for their hospitality, technical support and assistance.

REFERENCES

Aiba, H., Baba, K., and Matsukawa, M. 2010. A new species of *Stegodon* (Mammalia, Proboscidea) from the Kazusa Group (lower Pleistocene), Hachioji City, Tokyo, Japan and its evolutionary morphodynamics. Palaeontology, 53:47–490. https://doi.org/10.1111/j.1475-4983.2010.00953.x

Aitken, M.J. 1998. An Introduction to Optical Dating: the Dating of Quaternary Sediments by the Use of Photon-Stimulated Luminescence. Oxford University Press, Oxford, United Kingdom. https://doi.org/10.1093/oso/9780198540922.001.0001

An, Z., Gao, W., Zhu, Y., Kan, X., Wang, J., Sun, J., and Wei, M. 1990. Magnetostratigraphic dates of Lantian *Homo erectus*. Acta Anthropologica Sinica, 9:1–7.

Ancrenaz, M., Oram, F., Nardiyono, N., Silmi, M., Jopony, M.E.M., Voigt, M., Seaman, D.J.I., Sherman, J., Lackman, I., Traeholt, C., Wich, S.A., Santika, T., Struebig, M.J., and Meijaard, E. 2021. Importance of small forest fragments in agricultural landscapes for maintaining orangutan metapopulations. Frontiers in Forests and Global Change, 4:560944. https://doi.org/10.3389/ffgc.2021.560944

Ao, H., Zhang, P., Dekkers, M.J., Roberts, A.P., Zhinseng A., Yongxiang L., Fengyan L., Lin S., and Li, X. 2016. New magnetochronology of Late Miocene mammal fauna, NE Tibetan Plateau, China: mammal migration and paleoenvironments. Earth and Planetary Science Letters, 434:220–230. https://doi.org/10.1016/j.epsl.2015.11.019

Arambourg, C. and Fromaget, J. 1938. Le gisement quaternaire de Tam Nang (Chaîne Annamitique septentrionale). Sa stratigraphie et ses faunes. Comptes Rendus de l'Academie des Sciences, 207:793–795.

Aslam, S., Iqbal, A., Khan, A., Akbar khan, M., and Akhtar, M. 2015. New fossil remains of *Stegodon bombifrons* (Proboscideans) from the Pinjor Stage Soan Formation of Pakistan. Biologia (Lahore, Pakistan), 61:101–106.

Bacon, A.M., Demeter, F., Tougard, C., de Vos, J., Sayavongkhamdy, T., Antoine, P.O., Bouasisengpaseuth, B., and Sichanthongtip, P. 2008. Redécouverte d'une faune Pléistocène dans les remplissages karstiques de Tam Hang au Laos: premiers résultats. Comptes Rendus Palevol, 7:277–288. https://doi.org/10.1016/j.crpv.2008.03.009

Bacon, A.M., Duringer, P., Antoine, P.O., Demeter, F., Shackelford, L., Sayavongkhamdy, T., Sichanthongtip, P., Khamdalavong, P., Nokhamaomphu, S., Sysuphanh, V., Patole-Edoumba, E., Chabaux, F., and Pelt, E. 2011. The Middle Pleistocene mammalian fauna from Tam Hang karstic deposit, northern Laos: new data and evolutionary hypothesis. Quaternary International, 245:315–332. https://doi.org/10.1016/j.quaint.2010.11.024

Bacon A.M., Demeter, F., Duringer, P., Patole-Edoumba, E., Sayavongkhamdy, T., Coupey, A.S., Shackelford, L., Westaway, K.E., Ponche, J.L., Antoine, P.O., and Sichanthongtip, P. 2012. Les sites de Tam Hang, Nam Lot et Tam Pà Ling au nord du Laos: des gisements à vertébrés du Pléistocène aux origines des hommes modernes. CNRS Editions:149.

Bacon, A.M., Westaway, K.E., Antoine, P.O., Duringer, P., Blin, A., Demeter, F., Ponche, J.L., Zhao, J.X., Barnes, L.M., Sayavonkhamdy, T., Thuy, N.T.K., Long, V.T., Patole-Edoumba, E., and Shackelford, L. 2015. Late Pleistocene mammalian assemblages of Southeast Asia: new dating, mortality profiles and evolution of the predator–prey relationships in an environmental context. Palaeogeography, Palaeoclimatology, Palaeoecology, 422:101-127. https://doi.org/10.1016/j. palaeo.2015.01.011

Bacon, A.M., Bourgon, N., Dufour, E., Zanolli, C., Duringer, P., Ponche, J.L., Antoine, P.O., Shackelford, L., Huong, N.T.M., and Sayavonkhamdy, T. 2018. Nam lot (MIS 5) and Duoi U'Oi (MIS 4) Southeast Asian sites revisited: zooarchaeological and isotopic evidences. Palaeogeography, Palaeoclimatology, Palaeoecology, 512:132–144. https://doi.org/10.1016/j.palaeo.2018.03.034

Batchelor, B.C. 1979a. Discontinuously rising Late Cainozoic eustatic sea-levels with special reference to Sundaland, Southeast Asia. Geologie en Mijnbouw, 58:1–20. https://doi.org/10.1016/0198-0254(79)90729-5

Batchelor, B.C. 1979b. Geological characteristics of certain coastal and offshore placers as essential guides for tin exploration in Sundaland, Southeast Asia. Bulletin of the Geological Society of Malaysia, 11:283–313. https://doi.org/10.7186/bgsm11197913

Batchelor, D.A. 2015. Clarification of stratigraphic correlation and dating of Late Cainozoic alluvial units in Peninsular Malaysia. Bulletin of the Geological Society of Malaysia, 61:75–84. https://doi.org/10.7186/bgsm61201508

Brennan, B.J. 2003. Beta doses to spherical grains. Radiation Measurements, 37:299–303. https://doi.org/10.1016/s1350-4487(03)00011-8

Bøtter-Jensen, L. and Mejdahl, V. 1988. Assessment of beta dose-rate using a GM multicounter system. International Journal of Radiation Applications and Instrumentation. Part D. Nuclear Tracks and Radiation Measurements, 14:187–191. https://doi.org/10.1016/1359-0189(88)90062-3

Chen, G. 1999. *Sinomastodon* Tobien, et al., 1986 (Proboscidea, Mammalia) from the Pliocene and Early–Middle Pleistocene of China. Proceedings of the Seventh Annual Meeting of the Chinese Society of Vertebrate Paleontology, Beijing, China, p. 179–187. (in Chinese with English summary)

Chen, G. 2021. Palaeovertebrata Sinica. Volume III Basal Synapsids and Mammals. Fascicle 10 (Serial No. 23) Hyracoidea and Proboscidea. Science Press, Beijing.

Cheng, H., Edwards, R.L., Shen, C.C., Polyak, V.J., Asmerom, Y., Woodhead, J., Hellstrom, J., Wang, Y.J., Kong, X., Spotl, C., Wang, X.F., and Alexander Jr., E. 2013. Improvements in ^{230}Th dating, ^{230}Th and ^{234}U half-life values, and U-Th isotopic measurements by multi-collector inductively coupled plasma mass spectrometry. Earth and Planetary Science Letters, 371–372:82–91. https://doi.org/10.1016/j.epsl.2013.04.006

Ciochon, R.L. 2009. The mystery ape of Pleistocene Asia. Nature, 459:910–911. https://doi.org/10.1038/459910a

Clift, W. 1828. On the fossil remains of two new species of *Mastodon*, and of other vertebrated animals, found on the left bank of the Irawadi. Transactions of the Geological Society of London, 2:369–376. https://doi.org/10.1144/transgslb.2.3.369

Colbert, E.H. 1943. Pleistocene vertebrates collected in Burma by the American Southeast Asia Expedition. Transactions of the American Philosophical Society, 32:395–429. https://doi.org/10.70249/9798893983203-006

Colbert, E.H. and Hooijer, D.A. 1953. Pleistocene mammals from the limestone fissures of Szechwan, China. Bulletin of the American Museum of Natural History, 10:7–134.

Corbet, G.B. and Hill, J.E. 1992. The Mammals of the Indomalayan Region. Oxford University Press, USA.

Cornivus, G. 1988. The Mio–Plio–Pleistocene litho- and biostratigraphy of the Surai Khola Siwaliks in West Nepal: first results. Comptes Rendus de l'Académie des Sciences Paris, 306:1471–1477.

Cuong, N.L. 1985. Fossile menschenfunde aus nordvietnam, p. 96–102. In Herrmann J. and Ullrich, H. (eds.), Menschwerdung–Biotischer und Gesellschaftlicher Entwicklungsprozess. Akademieverlag, Berlin, Germany.

Davison, G.W.H. 1994. Some remarks on vertebrate remains from the excavation at Gua Gunung Runtuh, Perak, p. 141–148. In Majid, Z. (ed.), The Excavation of Gua Gunung Runtuh and the Discovery of the Perak Man in Malaysia. Department of Museums and Antiquity Malaysia, Kuala Lumpur.

Delfino, M. and de Vos, J. 2010. A revision of the Dubois crocodylians, *Gavialis bengawanicus* and *Crocodylus ossifragus*, from the Pleistocene *Homo erectus* beds of Java. Journal of Vertebrate Paleontology, 30:427–441. https://doi.org/10.1080/02724631003617910

de Vos, J. 1995. The migration of *Homo erectus* and *Homo sapiens* in South East Asia and the Indonesian archipelago, p. 239–260. In Bower, J.R.F and Sartono, S. (eds.), Human Evolution on the Ecological Context, Volume I, Evolution and Ecology of *Homo erectus*. Pithecanthropus Centennial Foundation, Leiden University, Netherlands.

de Vos, J. 2007. Vertebrate records: Mid-Pleistocene of southern Asia, p. 3232–3249. In Elias, S.A. (ed.), Encyclopedia of Quaternary Science. Elsevier, Oxford. https://doi.org/10.1016/b0-44-452747-8/00256-8

de Vos, J. and Long, V.T. 1993. Systematic discussion of the Lang Trang fauna. Unpublished report.

de Vos, J. and Long, V.T. 2001. First settlements: relations between continental and insular Southeast Asia, p. 225–249. In Sémah, F., Falguères, C., Grimaud-Hervé, D., and Sémah, A.M. (eds.) Origine des Peuplements et Chronologie des Cultures Paléolithiques dans le Sud-Est Asiatique. Semenanjung/Artcom, Paris.

de Vos, J., van den Hoek Ostende, L.W., and van den Bergh, G.D. 2007. Patterns in insular evolution of mammals: a key to island palaeogeography, p. 315–345. In Renema, W. (ed.), Biogeography, Time and Place: Distributions, Barriers and Islands. Springer, Dordrecht, Netherlands. https://doi.org/10.1007/978-1-4020-6374-9_10

Dietrich, W.O. 1926. Zur Altersbestimmung der *Pithecanthropus* Schichten. Sitzungsberichte der Gesellschaft Naturforschender Freunde zu Berlin for 1924, p. 134–139.

Duangkrayom, J., Nishioka, Y., Saokan, C., Jintasakul, P., Thungprue, N., and Worawansongkham, R. 2017. Proboscidean fossils (Mammalia) from the Quaternary deposits on *Stegodon* Cave, Thungwa, Satun Province, southern Thailand. Waseda Institute for Advanced Study Discussion Paper, No.2018-001:1–19.

Dubois, E. 1908. Das geologischer Alter der Kendeng- oder Trinil-Fauna. Tijdschrift van het Koninklijk Nederlandsch Aardrijskunding Genootschap, 2:1235–1270.

Edwards, R.L., Chen, J.H., and Wasserburg, G.J. 1987. ^{238}U–^{234}U–^{230}Th–^{232}Th systematics and the precise measurement of time over the past 500,000 years. Earth and Planetary Science Letters, 81:175–192. https://doi.org/10.1016/0012-821X(87)90154-3

Falconer, H. 1857. On the species of *Mastodon* and elephant occurring in the fossil state in Great Britain, Part I, *Mastodon*. Quarterly Journal of the Geological Society of London, 13: 307–360. https://doi.org/10.1144/gsl.jgs.1857.013.01-02.43

Falconer, H. and Cautley, P.T. 1846. Fauna Antiqua Sivalensis, Part I, Proboscidea. Smith, Elder and Co., London. https://doi.org/10.5962/bhl.title.61447

Foster, B.L. 2017. On the discovery of cementum. Journal of Periodontal Research, 52: 666–685. https://doi.org/10.1111/jre.12444

Ghani, A.A., Searle, M., Robb, M.L., and Sun-Lin Chung, S. 2013. Transitional I S type characteristic in the Main Range Granite, Peninsular Malaysia. Journal of Asian Earth Sciences, 76:225–240. https://doi.org/10.1016/j.jseaes.2013.05.013

Guérin, G., Mercier, N., and Adamiec, G. 2011. Dose rate conversion factors: update. Ancient TL, 29:5–11. https://doi.org/10.26034/la.atl.2011.443

Hassan, K., Nakamura, T., Price, D.M., Woodroffe, C.D., and Fujii, S. 1993. Radiocarbon and thermoluminescence dating of the Old Alluvium from a coastal site in Perak, Malaysia. Sedimentary Geology, 83:199–210. https://doi.org/10.1016/0037-0738(93)90013-u

Henri, F. and Amnan, I. 1994. Biostratigraphy of Kinta Valley. Bulletin of the Geological Society of Malaysia, 58:159–172. https://doi.org/10.7186/bgsm38199515

Hilgen, S.L., Pop, E., Adhityatama, S., Veldkamp, T.A., Berghuis, H.W.K., Sutisna, I., Yur-naldi, D., Dupont-Nivet, G., Reimann, T., Nowaczyk, N., Kuiper, K.F., Krijgsman, W., Vonhof, H.B., Ekowati, D.R., Alink, G., Hafsari, N.L.G.D.M., Drespriputra, O., Verpoorte, A., Bos, R., Simanjuntak, T., Prasetyo, B., and Joordens, J.C.A. 2023. Revised age and stratigraphy of the classic *Homo erectus*-bearing succession at Trinil (Java, Indonesia). Quaternary Science Reviews, 301:107908. https://doi.org/10.1016/j.quascirev.2022.107908

Hooijer, D.A. 1954. Pleistocene Vertebrates from Celebes XI. Molars and a tusked mandible of *Archidiskodon celebensis* Hooijer. Zoologische Mededelingen, 33:103–120.

Hooijer, D.A. 1955. Fossil Proboscidea from the Malay Archipelago and India. Zoologische Verhandelingen, 28:1–146.

Hooijer, D.A. 1962. Report upon a collection of Pleistocene mammals from tin-bearing deposits in a limestone cave near Ipoh, Kinta Valley, Perak. Federation Museums Journal, 7:1–5.

Huntley, D.J. and Baril, M.R. 1997. The K content of the K-feldspars being measured in optical dating or in thermoluminescence dating. Ancient TL, 15:11–13. https://doi.org/10.26034/la.atl.1997.271

Huntley, D.J. and Hancock, R. 2001. The Rb contents of the K-feldspar grains being measured in optical dating. Ancient TL, 19:43–46. https://doi.org/10.26034/la.atl.2001.333

Hutt, G., Jaek, I., and Tchonka, J. 1988. Optical dating: K-feldspars optical response stimulation spectra. Quaternary Science Reviews, 7:381–385. https://doi.org/10.1016/0277-3791(88)90033-9

Ibrahim, K.I., Lim, T.T., Westaway, K.E., of Cranbrook, E., Humphrey, L., Muhammad, R.F., and Peng, L.C. 2013. First discovery of Pleistocene orangutan (*Pongo* sp.) fossils in Peninsular Malaysia: biogeographic and paleoenvironmental implications. Journal of Human Evolution, 65:770–797. https://doi.org/10.1016/j.jhevol.2013.09.005

Ishlahuda, H.S., Lim, T.T., Muhammad, R.F., Nur, S.I.A.T., and Mohammad, A.A.A. 2019. First systematic study of Late Pleistocene rat fossils from Batu Caves: new record of extinct species and biogeography implications. Sains Malaysiana, 48:2613–2622. https://doi.org/10.17576/jsm-2019-4812-02

Ingicco, T., van den Bergh, G.D., Jago-on, C., Bahain, J.-J., Chacón, M.G., Amano, N., Forestier, H., King, C., Manalo, K., Nomade, S., Pereira, A., Reyes, M. C., Semah, A. M., Shao, Q., Voinchet, P., Falgueres, C., Albers, P.C.H., Lising, M., Lyras, G., Yurnaldi, D., Rochette, P., Bautista, A., and de Vos, J. 2018. Earliest known hominin activity in the Philippines by 709 thousand years ago. Nature, 557:233–237. https://doi.org/10.1038/s41586-018-0072-8

Jaffey, A.H., Flynn, K.F., Glendenin, L.E., Bentley, W.C., and Essling, A.M. 1971. Precision measurement of half-lives and specific activities of ^{235}U and ^{238}U. Physical Review C, 4:1889–1906. https://doi.org/10.1103/PhysRevC.4.1889

Janensch, W. 1911. Die Proboscidier-Schaedel der Trinil-Expeditions-Sammlung, p. 151–195. In Selenka, L. and Blanckenhorn, M. (eds.), Die *Pithecanthropus*-Schichten auf Java. Leipzig, Engelmann. https://doi.org/10.5962/bhl.title.60936

Jensen, B.J.L., Dufrane, A., Mark, D., Zaim, Y., Rizal, Y., Aswan, A., Hascary, A., Ciochon, R., Gunnell, G., Larick, R., and Zonneveld, J.P. 2017. Newly described tephra provide age constraints to *Stegodon* fossils in west (Indonesian) Timor. American Geophysical Union, Fall Meeting.

Joordens, J.C.A., d'Errico, F., Wesselingh, F.P., Munro, S., de Vos, J., Wallinga, J., Ankjærgaard, C., Reimann, T., Wijbrans, J.R., Kuiper, K.F., Mücher, H.J., Coqueugniot, H., Prié, V., Joosten, I., van Os, B., Schulp, A.S., Panuel, M., van der Haas, V., Lustenhouwer, W., Reijmer, J.G.J., and Roebroeks, W. 2015. *Homo erectus* at Trinil on Java used shells for tool production and engraving. Nature, 518:228–231. https://doi.org/10.1038/nature13962

Kahlke, H.D. 1961. On the complex of the *Stegodon-Ailuropoda* fauna of southern China and the chronological position of *Gigantopithecus blacki* v. Koenigswald. Vertebrata PalAsiatica, 6:83–108.

Kha, L.T. 1976. First remarks on the Quaternary fossil fauna of northern Vietnam. Vietnamese Studies, 46:107–126.

Kikinis, R., Pieper, S.D., and Vosburgh, K.G. 2014. 3D slicer: a platform for subject-specific image analysis, visualization, and clinical support, p. 277–289. In Jolesz, F. (ed.), Intraoperative Imaging and Image-Guided Therapy. Springer, New York. https://doi.org/10.1007/978-1-4614-7657-3_19

Konishi, S. and Yoshikawa, S. 1999. Immigration times of the two proboscidean species, *Stegodon orientalis* and *Palaeoloxodon naumanni*, into the Japanese islands and the formation of land bridge. Earth Science (Chikyu Kagaku), 53:125–134 (in Japanese).

Kundal, S., Bhadur, G., and Kumar, S. 2017. A Late Pliocene baby *Stegodon* cf. *Stegodon insignis (*Proboscidea) from Upper Siwalik of Samba District, Jammu and Kashmir, India. Earth Science India, 10:82–93.

Lambard, J., Pereira, A., Voinchet, P., Guillou, H., Reyes, M.C., Nomade, S., Gallet, X., Belarmino, M., Bahain, J., de Vos, J., Falguères, C., Cosalan, A., and Ingicco, T. 2024. Geochronological advances in human and proboscideans first arrival date in the Philippines archipelago (Cagayan valley, Luzon Island). Quaternary Geochronology, 84:101597. https://doi.org/10.1016/j.quageo.2024.101597

Lim, T.T. 2013. Quaternary *Elephas* from Peninsular Malaysia: historical overview and new material. Raffles Bulletin of Zoology, Supplement No. 29:139–153.

Lin, C.C. 1963. Geology and ecology of Taiwan prehistory. Asian Perspectives, 7:203–213.

Long, V.T. and Du, H.V. 1981. Zoological species belonging to the Pleistocene and the geochronology of sediments containing them in caves and grottos in northern Viet Nam. Khao Co Hoc, 1:16–19 (in Vietnamese).

Long, V.T., de Vos, J., and Ciochon, R.S. 1996. The fossil mammal fauna of the Lang Trang caves, Vietnam, compared with Southeast Asian fossil and recent mammal faunas: the geographical implications. Bulletin of the Indo-Pacific Prehistory Association, 14:101–109.

Louys, J., Curnoe, D., and Tong, H.W. 2007. Characteristics of Pleistocene megafauna extinctions in Southeast Asia. Palaeogeography, Palaeoclimatology, Palaeoecology, 243:152–173. https://doi.org/10.1016/j.palaeo.2006.07.011

Louys, J., Price, G.J., and O'Connor, S. 2016. Direct dating of Pleistocene *Stegodon* from Timor island, East Nusa Tenggara. PeerJ, 4:1788. https://doi.org/10.7717/peerj.1788

Louys, J., Zaim, Y., Rizal, Y., Aswan, Puspaningrum, M., Trihascaryo, A., Price G.J., Petherick, A., Scholtz, E., and DeSantis, L.R.G. 2021. Sumatran orangutan diets in the Late Pleistocene as inferred from dental microwear texture analysis. Quaternary International, 603:74–81. https://doi.org/10.1016/j.quaint.2020.08.040

Louys, J., Duval, M., Price, G.J., Westaway, K., Zaim, Y., Rizal, Y., Aswan, Puspaningrum, M., Trihascaryo, A., Breitenbach, S.F.M., Kwiecien, O., Cai, Y., Higgins, P., Albers, P.C.H., de Vos, J., and Roberts, P. 2022. Speleological and environmental history of Lida Ajer cave, western Sumatra. Philosophical Transactions of the Royal Society of London. Series B, Biological Sciences, 377:20200494. https://doi.org/10.1098/rstb.2020.0494

Ma, A. and Tang, H. 1992. On discovery and significance of a Holocene *Ailuropoda-Stegodon* fauna from Jinhua, Zhejiang. Vertebrata PalAsiatica, 30:295–312.

Maglio, V.J. 1973. Origin and evolution of the Elephantidae. Transactions of the American Philosophical Society New Series, 63:1–149. https://doi.org/10.2307/1006229

Makiyama, J. 1938. Japonic Proboscidea. Memoirs of the College of Science, Kyoto Imperial University, Series B, 14:1–59.

Marwick, B. 2009. Biogeography of Middle Pleistocene hominins in mainland Southeast Asia: a review of current evidence. Quaternary International, 202:51–58. https://doi.org/10.1016/j.quaint.2008.01.012

Muhammad, R.F. 2010. The geomorphology and origin of Gua Tempurung, Perak, west Malaysia. Bulletin of the Geological Society of Malaysia, 56:127–132. https://doi.org/10.7186/bgsm56201018

Muhammad, R.F. 2018. The extreme karstification of Kinta Valley Karst, west Malaysia. Proceedings of the 15th Multidisciplinary Conference on Sinkholes and the Engineering and Environmental Impacts of Karst and the 3rd Appalachian Karst Symposium, p. 297–305. https://doi.org/10.5038/9780991000982.1063

Muhammad, R.F. and Yeap, E.B. 2000. Proposed conservation of Badak Cave C, Lenggong as extraordinary vertebrate fossil site. Proceeding Geological Society Malaysia Annual Geological Conference, Pulau Pinang, Malaysia, p. 189–196.

Muhammad, R.F., Yoshida, D., Tani, A, and Smart, P.L. 2002. Implications of Electron Spin Resonance and Uranium-series dating techniques on speleothems in the Kinta and Lenggong Valleys, west Malaysia. Advances in ESR Applications, 18:19–26.

Muhammad, R.F., Lim, T.T., Sahak, I.H., Azhar, N.N K., Razif, F.M., Hassan, M.H.A., Basir, M.L., Mamat, M.R., Zin, M.Z.A.N., and Zoo, S. 2019. High potential new Quaternary fossil cave sites in Merapoh (Pahang), with new geographic records for orangutan and Asian black bear. Warta Geologi, 45:400–404. https://doi.org/10.7186/wg454201903

Muhammad, R.F., Lim T.T, Ibrahim, N., Razak, M.A.A., Razif, F.M, Kem, Z., Ching, B.T., Tee C.Y., Nang, Y.L., Chan, J.C., Chan, J.F., Rahman, M.N.A., and Hussein, S.R. 2020. First discovery of *Stegodon* (Proboscidea) in Malaysia. Warta Geologi, 46:196–198. https://doi.org/10.7186/wg463202004

Nanda, A.C. 1980. A new species of *Stegodon* from the Upper Siwalik subgroup of Ambala, India. Geological Survey of India, Special Publication, 11:365–370.

Naumann, E. 1890. *Stegodon mindanensis,* eine neue Art von Uebergangs-Mastodonten. Zeitschrift der Deutschen Geologischen Gesellschaft, 42: 166–169.

Olsen, J.W. and Ciochon, R.L. 1990. A review of evidence for postulated Middle Pleistocene occupations in Viet Nam. Journal of Human Evolution, 19:761–788. https://doi.org/10.1016/0047-2484(90)90020-c

Oram, F. 2018. Abundance, feeding and behavioural ecology of orangutans *(Pongo pygmaeus morio)* in the fragmented forests of the Kinabatangan floodplain. Unpublished PhD Thesis, University Malaysia Sabah (ITBC), Kota Kinabalu, Sabah, Malaysia.

O'Regan, H.J., Bishop, L., Lamb, A., Elton, S., and Turner, A. 2005. Large mammal turnover in Africa and the Levant between 1.0 and 0.5 Ma. Geological Society, London, Special Publications, 247:231–249. https://doi.org/10.1144/gsl.sp.2005.247.01.13

Osborn, H.F. 1929. New Eurasiatic and American proboscideans. American Museum Novitates, 393:1–23.

Osborn, H.F. 1942. Proboscidea: A Monograph of the Discovery, Evolution, Migration and Extinction of the Mastodonts and Elephants of the World. Volume II: Stegodontoidea, Elephantoidea. The American Museum Press, New York.

Otsuka, H. 1984. Stratigraphic position of the Chochen Vertebrate Fauna of the T'ouk'oushan Group in the environs of the Chochen district, southwest Taiwan, with special references to its geologic age. Journal of the Taiwan Museum, 37:37–56.

Puspaningrum, M.R., van den Bergh, G.D., Chivas, A.R., Setiabudi, E., and Kurniawan, I. 2020. Isotopic reconstruction of Proboscidean habitats and diets on Java since the Early Pleistocene: implications for adaptation and extinction. Quaternary Science Reviews, 228:106007. https://doi.org/10.1016/j.quascirev.2019.106007

Prescott, J.R. and Hutton, J.T. 1994. Cosmic ray contributions to dose rates for luminescence and ESR dating: large depths and long-term time variations. Radiation Measurements,

23:497–500.
https://doi.org/10.1016/1350-4487(94)90086-8

Rink, W.J., Wei, W., Bekken, D., and Jones, H.L. 2008. Geochronology of *Ailuropoda-Stegodon* fauna and *Gigantopithecus* in Guangxi province, southern China. Quaternary Research, 69:377–387.
https://doi.org/10.1016/j.yqres.2008.02.008

Rizal, Y. Westaway, K.E., Zaim, Y., van den Bergh G.D., Bettis E.A., Morwood, M.J., Huffman, O.F., Grün, R., Joannes-Boyau, R., Bailry, R.M., Sidarto, Westaway, M.C., Kurniawan, I., Moore, M.W., Storey, M., Aziz, F., Suminto, Zhao, J., Aswan, Sipola, M.E., Larick, R., Zonneveld, J., Scott, R., Putt, S., and Ciochon R.L. 2020. Last appearance of *Homo erectus* at Ngandong, Java, 117,000–108,000 years ago. Nature, 577:381–385.
https://doi.org/10.1038/s41586-019-1863-2

Roth, V.L. and Shoshani, J. 1988. Dental identification and age determination in *Elephas maximus*. Journal of Zoology (London), 214:567–588.
https://doi.org/10.1111/j.1469-7998.1988.tb03760.x

Sabah Wildlife Department. 2020. Orangutan Action Plan for Sabah 2020-2029. Kota Kinabalu, Sabah, Malaysia.

Saegusa, H. 1996. Stegodontidae: evolutionary relationships, p. 178–190. In Shoshani, J. and Tassy, P. (eds.), The Proboscidea: Evolution and Paleoecology of Elephants and Their Relatives. Oxford University Press, Oxford, United Kingdom.
https://doi.org/10.1093/oso/9780198546528.003.0018

Saegusa, H. 2001. Comparisons of *Stegodon* and Elephantid abundances in the Late Pleistocene of southern China. Proceedings of the First International Congress, Rome, p. 345–349.

Saegusa, H., Thasod, Y., and Ratanasthien, B. 2005. Notes on Asian stegodontids. Quaternary International, 126–128:31–48.
https://doi.org/10.1016/j.quaint.2004.04.013

Schepartz, L.A., Stoutamire S., and Bekken, D.A. 2005. *Stegodon orientalis* from Panxian Dadong, a Middle Pleistocene archaeological site in Guizhou, South China: taphonomy, population structure and evidence for human interactions. Quaternary International, 126–128:271-282.
https://doi.org/10.1016/j.quaint.2004.04.026

Sharma, C.K. and Singh, Y.L. 1966. Two vertebrate fossils from Nepal. Unpublished report, Nepal Bureau of Mines, Lainchaur, Kathmandu, Nepal.

Shen, C.C., Edwards, R.L., Cheng, H., Dorale, J.A., Thomas, R.B., Moran, S.B., Weinstein, S.E., and Edmonds, H.N. 2002. Uranium and thorium isotopic and concentration measurements by magnetic sector inductively coupled plasma mass spectrometry. Chemical Geology, 185:165–178.
https://doi.org/10.1016/s0009-2541(01)00404-1

Shen, C.C., Wu, C.C., Cheng, H., Edwards, R.L., Hsieh, Y.T., Gallet, S., Chang, C.C., Li, T.Y., Lam, D.D., Kano, A., Hori, M., and Spotl, C. 2012. High-precision and high-resolution carbonate ^{230}Th dating by MC-ICP-MS with SEM protocols. Geochimica et Cosmochimica Acta, 99:71–86.
https://doi.org/10.1016/j.gca.2012.09.018

Shikama, T. 1936. On the genus *Parastegodon*. Transactions and Proceedings of the Palaeontological Society of Japan, 4:62–69.
https://doi.org/10.5575/geosoc.43.557

Shikama, T., Otsuka, H., and Tomida, Y. 1975. Fossil Proboscidea from Taiwan. Science Reports of Yokohama National University, 2:13–62.

Sondaar, P.Y. 1984. Faunal evolution and the mammalian biostratigraphy of Java. Courrier Forschung Senckenberg, 69:219–235.

Stauffer, P.H. 1973. Cenozoic, p. 143–176. In Gobbett, D.J. and Hutchison, C.S. (eds.), Geology of the Malay Peninsula (West Malaysia and Singapore). Wiley-Interscience, New York.

Storm, P., Aziz, F., de Vos, J., Kosasih, D., Baskoro, S., Ngaliman, and van den Hoek Ostende, L.W. 2005. Late Pleistocene *Homo sapiens* in a tropical rainforest fauna in east Java. Journal of Human Evolution, 49:536–545.
https://doi.org/10.1016/j.jhevol.2005.06.003

Suraprasit, K., Jaeger, J.J., Chaimanee, Y., Chavasseau, O., Yamee, C., Tian, P., and Panha, S., 2016. The Middle Pleistocene vertebrate fauna from Khok Sung (Nakhon Ratchasima,

Thailand): biochronological and paleobiogeographical implications. ZooKeys, 613:1–157. https://doi.org/10.3897/zookeys.613.8309
Takahashi, K. and Chang, C.H. 2001. Proboscidean fossils from the Japanese archipelago and Taiwan islands and their relationship with the Chinese mainland. The World of Elephants – International Congress, Rome, p. 148–151.
Takai, M., Saegusa, H., Htike, T., and Maung-Thein, Z. 2006. Neogene mammalian fauna in Myanmar. Asian Paleoprimatology, 4:143–172.
Tjia, H.D. 2000. A large vertebrate fossil at Naga Mas Cave, Bukit Lanno, Kinta Valley, p. 209–218. In series, Warisan Geologi Malaysia 3. Resource Development for Conservation and Nature Tourism. Lestari, Universiti Kebangsaan Malaysia, Malaysia.
Tong, H. and Liu, J. 2004. The Pleistocene-Holocene extinctions of mammals in China, p. 111–119. In Dong, W. (ed.), Proceedings of the Ninth Annual Symposium of the Chinese Society of Vertebrate Paleontology. China Ocean Press, Beijing.
Tong, H. and Patou-Mathis, M. 2003. Mammoth and other proboscideans in China during the Late Pleistocene. Deinsea, 9:421–428.
Tougard, C. 1998. Les faunes de grands mammifères du Pléistocène moyen terminal de Thaïlande dans leur cadre phylogénétique, paléoécologique et biochronologique. Unpublished PhD Dissertation, Université de Montpellier II, Montpellier, France.
Tougard, C. 2001. Biogeography and migration routes of large mammal faunas in South-East Asia during the Late Middle Pleistocene: focus on the fossil and extant faunas from Thailand. Palaeogeography, Palaeoclimatology, Palaeoecology, 168:337–358. https://doi.org/10.1016/S0031-0182(00)00243-1
Turvey, S., Tong, H., Stuart, A., and Lister, A. 2013. Holocene survival of Late Pleistocene megafauna in China: a critical review of the evidence. Quaternary Science Reviews, 76:156–166. https://doi.org/10.1016/j.quascirev.2013.06.030
van den Bergh, G.D. 1999. The Late Neogene elephantoid-bearing faunas of Indonesia and their palaeozoogeographic implications: a study of the terrestrial faunal succession of Sulawesi, Flores, and Java, including evidence for early hominid dispersal east of Wallace's Line. Scripta Geologica, 117:1–419.
van den Bergh, G., de Vos, J., Aziz, F., and Morwood, M.J. 2001a. Elephantoidea in the Indonesian region: new *Stegodon* findings from Flores. Proceedings of the First International Congress, Rome, p. 623–627
van den Bergh, G., de Vos, J., and Sondaar, P. 2001b. The Late Quaternary palaeogeography of mammal evolution in the Indonesian Archipelago. Palaeogeography, Palaeoclimatology, Palaeoecology, 171:385–408. https://doi.org/10.1016/S0031-0182(01)00255-3
van den Bergh, G.D., Rokhus D.A., Morwood, M.J., Sutikna, T., Jatmiko, and Saptomo, E.W. 2008. The youngest *Stegodon* remains in Southeast Asia from the Late Pleistocene archaeological site Liang Bua, Flores, Indonesia. Quaternary International, 182:16– 48. https://doi.org/10.1016/j.quaint.2007.02.001
van der Geer, A.A.E., van den Bergh, G.D., Lyras, G.A., Prasetyo, U.W., Due, R.A., Setiyabudi, E., and Drinia, H. 2016. The effect of area and isolation on insular dwarf proboscideans. Journal of Biogeography, 43:1656–1666. https://doi.org/10.1111/jbi.12743
von Koenigswald, G.H.R. 1933. Beitrag zur Kenntnis der fossilen Wirbeltiere Javas. Dienst van den Mijnbouw Nederlandsch-Indië: Wetenschappelikke MededeelingenI. Teil, 23:1–127.
von Koenigswald, G.H.R. 1935. Die fossilen Saugertier Fauna Javas. Proceeding Koninklijke Nederlandsche Akademie van Wetenschappen, 38:188–198.
Walker, D. 1956. Studies on the Quaternary of the Malay Peninsula 1: alluvial deposits of Perak and the relative levels of land and sea. Federation Museums Journal, 1 and 2:19–34.
Wang, W. and Xia, J. 1991. The measurement of annual dose from Th series and U-series decay chains by thick source alpha counting. Nuclear Techniques, 14:101–108.
Wang, W., Potts, R., Baoyin, Y., Huang, W., Cheng, H., Edwards, R.L., and Ditchfield, P. 2007. Sequence of mammalian fossils, including hominoid teeth, from the Bubing Basin caves, South China. Journal of Human Evolution, 52:370–379. https://doi.org/10.1016/j.jhevol.2006.10.003
Wang, W., Liao, W., Li, D., and Tian, F. 2014. Early Pleistocene large-mammal fauna associated with *Gigantopithecus* at Mohui Cave, Bubing Basin, South China. Quaternary International,

354:122–130.
https://doi.org/10.1016/j.quaint.2014.06.036

West, R.M. and Munthe, J. 1981. Neogene vertebrate palaeontology and stratigraphy of Nepal. Nepal Geological Society, 1:1–14.
https://doi.org/10.3126/jngs.v1i1.32664

Westaway, K., Morwood, M., Roberts, R., Rokus, A.D., Zhao, J., Storm, P., Aziz, F., van den Bergh, G., Hadi, P., Jatmiko, and de Vos, J. 2007. Age and biostratigraphic significance of the Punung Rainforest Fauna, East Java, Indonesia, and implications for *Pongo* and *Homo*. Journal of Human Evolution, 53:709–717.
https://doi.org/10.1016/j.jhevol.2007.06.002

Wich, S.A., Meijaard, E., Marshall, A.J., Husson, S., Ancrenaz, M., Lacy, R.C., van Schaik, C.P., Sugardjito, J., Simorangkir, T., Traylor-Holzer, K., Doughty, M., Supriatna, J., Dennis, R., Gumal, M., Knott, C.D., and Singleton, I. 2008. Distribution and conservation status of the orang-utan (spp.) on Borneo and Sumatra: how many remain? Oryx, 42:329-339.
https://doi.org/10.1017/s003060530800197x

Zeitoun, V., Seveau, A., Forestier, H., Thomas, H., Lenoble, A., Laudet, F., Antoine, P.O., Debruyne, R., Ginsburg, L., Mein, P., Winayalai, C., Chumdee, N., Doyasa, T., Kijngam, A., and Nakbunlung, S. 2005. Découverte d'un assemblage faunique à *Stegodon–Ailuropoda* dans une grotte du Nord de la Thaïlande (Ban Fa Suai, Chiang Dao). Comptes Rendus Palevol, 4:255–264.
https://doi.org/10.1016/j.crpv.2004.11.013

Zeitoun, V., Lenoble, A., Laudet, F., Thompson, J., Rink, W.J., Mallye, J.B., and Chinnawut, W. 2010. The Cave of the Monk (Ban Fa Suai, Chiang Dao wildlife sanctuary, northern Thailand). Quaternary International, 220:160–173.
https://doi.org/10.1016/j.quaint.2009.11.022

Zhang, H., Wang, Y., Janis, C.M., Goodall, R.H., Purnell, and M.A. 2017. An examination of feeding ecology in Pleistocene proboscideans from southern China *(Sinomastodon, Stegodon, Elephas),* by means of dental microwear texture analysis. Quaternary International, 445:60-70.
https://doi.org/10.1016/j.quaint.2016.07.011

Zin-Maung-Maung-Thein, Takai, M., Uno, H., Wynn, J.G., Egi, N., Tsubamoto, T.,Thaung-Htike, Aung-Naing-Soe, Maung-Maung, Nishimura, T., and Yoneda, M. 2011. Stable isotope analysis of the tooth enamel of Chaingzauk mammalian fauna (late Neogene, Myanmar) and its implication to paleoenvironment and paleogeography. Palaeogeography, Palaeoclimatology, Palaeoecology, 300:11–22.
https://doi.org/10.1016/j.palaeo.2010.11.016

Zolkurnian, H. 1998. Urutan kebudayaan Holosen di Lembah Lenggong. Unpublished Masters Thesis, University of Science Malaysia, Pulau Pinang, Malaysia.

Zong, G. 1995. On new material of *Stegodon* with recollections of the classification of *Stegodon* in China. Vertebrata PalAsiatica, 33:216–230.

Zuraina, M. 1994. The Excavation of Gua Gunung Runtuh and the Discovery of the Perak Man in Malaysia. Department of Museums and Antiquity Malaysia, Kuala Lumpur.